Launch Failure Recovery Strategies and Analyses

George Moore
Spokane, Washington
gsmooree50@comcast.net

Introduction and Overview

The early launch phases, particularly during the rotation, are the most dangerous periods of a winch launch and the most demanding on the pilot. The high translational and angular dynamics coupled with the close ground proximity make launch failures during this period critical safety of flight issues. Launch failure here means a loss in power from the towing cable. The most common reasons for such failures are a break in the cable/weak link system or a drive/motor failure. Generally a cable system failure is readily detectable, as it is sudden, but the power may fail abruptly or gradually for a drive/motor failure. Such gradual failures can be very insidious and, if the pilot is not very attentive, recovery may be delayed with disastrous consequences. Because detection of a launch failure can be such a complex issue, this paper will focus on the recovery from the point the pilot recognizes the failure and initiates recovery.

There is a generally held consensus that the proper launch failure recovery action is to immediately unload the glider to essentially a zero-G condition and, as the glider goes over the top, to let the nose continue to drop, allow airspeed to build, and then smoothly reload the wings and return to level flight. The following analyses generally validate this methodology but there are a number of qualitative aspects in the above recovery description that this analysis will provide both objective guidance and quantitative values for the height loss that may be expected, the airspeeds that will occur, and the G-loads the aircraft will experience. Some of these numbers can be sobering and reinforce the need for quick and decisive action to avoid aircraft damage and occupant injury.

While hopefully useful for pilots to gain an understanding of what is going on during a launch failure recovery of any glider, this paper also develops a very robust recovery technique that can be very effectively implemented if the glider has available an Angle-of-Attack (AoA) indicator. This analysis indicates operating the glider during the pullout at high AoAs is near optimal for recovery so long as the glider is not stalled. Previous discussions have identified the value of such an indicator during the rotation to warn of a too high rotation rate coupled with inadequate airspeed where an incipient stall, which could turn into a flick spin, is a risk. In addition, such an AoA indicator with an aural warning (Dynon Avionics makes such a visual/aural AoA indicator) could also potentially warn of a gradual power failure where the glider is approaching its loaded stall speed as an additional aide in launch failure detection. This potential triple usage reinforces the value of an AoA for ground launches and may provide more impetuous for the development and approval of cost effective AoA instruments for gliders. But again this paper can provide value for operations without an AoA indicator in emphasizing the importance of operations within a safe AAA (Airspeed, Altitude, Attitude) envelope and techniques to achieving this. Opportunities for safely employing rotation rates in excess of the BGA recommendations are identified but are not suggested for use with classic winches or gliders without AoA indicators.

The organization of this paper is as follows: The next section defines a set of launch failure recovery phases to provide a clear basis for the discussions to follow. Only portions of the recovery are addressed in this paper as is discussed in that section. The generally held consensus of proper recovery actions is presented and the qualitative nature of these guidelines is observed. Then a basis for quantitative analysis of the recovery is introduced which, if proper instrumentation were available, could actually be executed with great effectiveness. Rather than slowly build up through detailed analyses, reference results are immediately presented and interpreted constituting an executive summary. A brief section follows outlining opportunities to safely employ rotation rates that exceed current BGA recommendations when tension controlled winches and gliders with AoA indicators become available. Then a more detailed description of the models employed to obtain these results is presented. Once this basis is established, variations on the reference results are developed that explore the effects of the AoA employed, drag, stall speed, alternate pushover strategies, and density altitude. Interested readers can skip the theoretical development portions altogether and review just these variations if they are not interested in the underlying models. The really mathematical developments are contained in the Appendix for those that wish to fully understand the development.

Launch Failure Recovery Definitions and Constant AoA Recovery Strategy

To establish a common set of terminology and delineate the limits of this investigation, a model for launch failure recovery is now presented using the illustration of Figure 1.

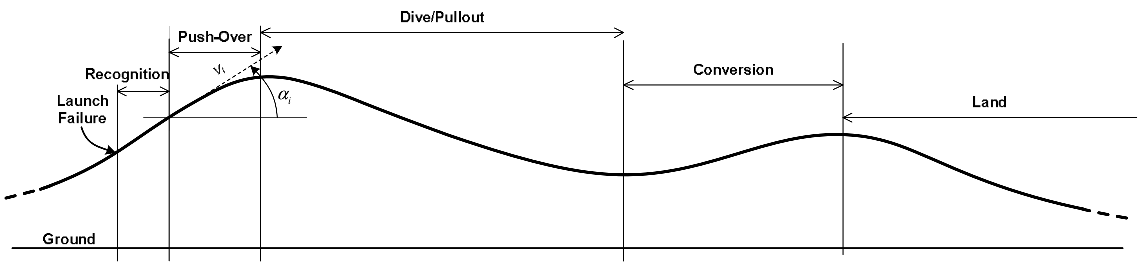

Figure 1. Launch Failure Recovery Phases Definitions

The five designated phases are Recognition, Pushover, Dive/Pullout, Conversion, and Land. As noted above, the Recognition Phase is not considered here other than to emphasize the importance of rapid recognition followed immediately by appropriate recovery actions. The starting point for this analysis is the Pushover Phase where the pilot transitions the trajectory to horizontal (but not necessarily with enough airspeed to establish gliding flight). V_i is the airspeed and α_i is the climb angle as recovery is initiated. The height at recovery initiation is the final input element for the AAA envelope. As the glider go over the top, it enters the Dive/Pullout Phase where the glider is accelerating due to gravity, and the wings are progressively reloaded. This reloading continues and the glider returns to horizontal flight now typically with an airspeed well in excess of that needed for gliding flight. During the Conversion Phase the pilot converts this excess airspeed back to height and/or deploys spoilers to dissipate this excess airspeed resulting in the glider descending at appropriate approach airspeed. The following Landing Phase is self-evident. This investigation does not consider the Conversion and Landing Phases in any detail. Assuming the glider has returned to level flight with a speed in excess of approach speed, there are a number of options for the last two phases depending on whether the decision is made to land straight ahead, make a 180° turn and land, or make an abbreviated circuit. The considerations for which is the most appropriate option are many and complex and are not addressed here. Again the situation of most concern here is where the failure is so low that landing straight ahead will generally be the only reasonable option. If the height after recovery is sufficient to consider the other options, the recovery was probably from an AAA condition that had plenty of margin to begin with.

Of paramount importance is to avoid stalling the aircraft during the recovery. Recovery from a stall at the low altitudes assumed here would be difficult if not impossible and the pullout height loss would be substantially increased. Obviously, if this increased loss results in impacting the ground before level flight is reestablished, the consequences can be dire. Even worse is the case where the stall results in a spin from which recovery would again be unlikely with catastrophic consequences. It is to this end that consensus holds that unloading the glider to a near zero-G condition for the Pushover Phase is preferred – an unloaded wing cannot be stalled. The physical sensation and indications (e.g. floating objects, seat belt straps…) of near weightlessness can be taught making effective application of this action possible. The investigation results support this course of action but, if it can be done safely, some technical merit to using some negative Gs during this period is also demonstrated. Further discussion of this variation is deferred until an initial analysis is completed.

Ignoring drag, fully unloading the aircraft will result in a ballistic trajectory and simple physics may be applied to determine the time to, the airspeed at, and the height gain to the ballistic trajectory peak relative to the point the pushover was initiated. This recovery initiation point is characterized by a velocity vector which includes the airspeed and the angle of climb and an entry altitude, the AAA combination. What will generally result is the glider trajectory being horizontal, at a reduced airspeed, and at some height over the point the pushover was initiated. This is the initial condition for the Dive/Pullout Phase entry.

Again consensus currently calls for allowing the trajectory to continue through horizontal into a dive to gain sufficient airspeed for the pullout. There are no definitive guidelines on how steep to dive and how much airspeed to attain before beginning the pullout nor how fast the wings should be reloaded. The guidelines are subjective and emphasize actions that avoid stalling during the pullout. With only an airspeed indicator, all that can be done is to insure the airspeed is sufficient that a stall is precluded for the G loads being applied. At an airspeed of 1.5 V_s, the wing can generate around 2.25 Gs before stalling. Holding 0 Gs and delaying the recovery until this airspeed is attained and then smoothly reloading the wings would generally be conservative with respect to stall avoidance. Even as the reloading is initiated, the airspeed will continue to increase until the bottom of the pullout so even more lift capability would build. [If a G-meter was available, the loaded stall speed could be inferred from the Gs being developed (the loaded stall speed increases with the square-root of the G load). If an analog G-meter is employed, the loaded stall speed for different G loads could be marked on the dial but things are happening so fast there would generally not be sufficient time for the pilot to read the G-meter stall speed and effectively compare it to the rapidly increasing airspeed. In addition, trying to fly the G-meter would keep the pilots head in the cockpit – not prudent this close to the ground. However, a mode of a flight computer with an acceleration and airspeed sensor could be developed that produced an aural/visual indication of how close the glider was to loaded stall speed. Note that this would not be applicable for stall avoidance during the launch when the cable is pulling. The proper solution is an AoA instrument – preferably with both aural and visual outputs.]

To analyze this problem further, some definitive quantitative method must be employed. If the glider had an AoA meter, one plausible method would be to fly the Dive/Pullout at a constant angle of attack. Assuming this angle is below the stall AoA, the wing could not be stalled regardless of the airspeed which satisfies the prime directive. Such a constant AoA pullout will be the basis for the analyses to follow. The second question is when to apply this AoA during the recovery. Initially we will consider applying it immediately as the glider goes over the top of the ballistic trajectory and later we will consider alternative points to begin reloading the wing. With this initial assumption, there is not an actual recovery dive element as the pullout technically begins immediately at the top of the ballistic trajectory. For the remainder of this discussion this phase will just be referred to as the Pullout Phase.

Summary Results for Constant AoA Launch Failure Recovery

The key results of employing this recovery behavior are illustrated using a plot showing representative recovery trajectories and a set of three contour plots. The recovery flight trajectories, in Figure 2, illustrate the glider path during the Pushover and Pullout Phases where the initial climb angle is 45^{o}. With a little reflection, these trajectories should appear very reasonable to most pilots. To simplify the application of these results to a broad range of gliders, the AoA is characterized, not by some number of degrees, but by relating it to common angles of attack employed in free-flight. These will be referenced to the AoAs that would sustain unaccelerated descending flight at different airspeeds referenced to the glider stall speed. The AoA employed for these reference trajectories is that associated with unaccelerated (steadily descending) flight at an airspeed of 1.5 V_s. The stall speed assumed is 20 m/s (38.9 knots) and the *L/D* employed is 20:1 representing drag losses. This AoA is commonly near the best *L/D* AoA and is a long way from stall AoA. Later in the paper, recoveries using an AoA of 1.3 V_s are considered. This AoA is commonly associated with minimum sink airspeed in level flight. The 1.5 V_s AoA is lower resulting in higher stall margins but the altitude required for recovery is shown to be higher. It is demonstrated shortly that the recovery requirements can be reduced using higher AoAs but, unless effective means of avoiding stall are available (e.g., an AoA indicator), the increased risks may outweigh the benefits. It was noted above that at 1.5 V_s the wing is capable of generating lift equal to 2.25 times the glider weight. But this would be using an AoA near stall. The AoA being employed here only would be generating 1 G in unaccelerated flight at that speed. The different traces represent airspeeds at the initiation of recovery varying from 0 to 85 knots (bottom trace to top) in increments of 5 knots. The axes are the horizontal and vertical positions of the glider relative to the point where recovery was initiated. No wind is assumed but a wind simply requires that this be interpreted relative to the moving airmass – it does not affect the height required for recovery to horizontal.

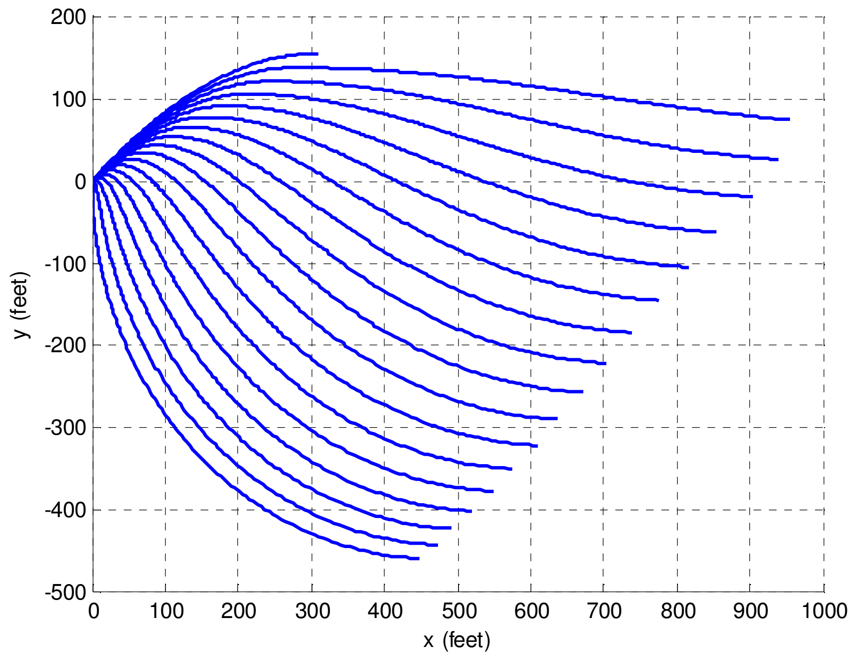

Figure 2. Recovery Trajectories: 1.5 V_s AoA, 45^o Attitude, V_s = 38.9 knots, *L/D* = 20:1.

It is almost implausible that any pilot would not recognize and begin recovery before the airspeed dropped below 40 knots, as the aircraft would likely have stalled, but these conditions are included for completeness. As the airspeed at initiation increases, the nearly ballistic portion of the recovery becomes clearly evident. In the top trace, for 85 knots, the airspeed at the top of the pushover is above 1.5 V_s (52.5 knots) and recovery is immediately complete at that point. For initial airspeeds greater than 72 knots, the recovery altitude, and indeed the entire recovery trajectory, is actually above the height at initiation although a short Pullout Phase is still present.

The contour plots are generated by running such trajectory simulations for hundreds of different combinations of initial airspeed and attitude. The axes of all these plots are the airspeed and attitude (more correctly, climb angle) at the moment recovery is initiated, i.e. the beginning of the Pushover Phase. The first contour plot presented is the most important. It indicates the amount of height lost, from the point the recovery is initiated, before the flight trajectory becomes horizontal with enough airspeed to generate a 1G lift factor or greater. With the assumed AoA, this airspeed is 1.5 V_s. Conceptually, if the glider altitude, at the moment recovery actions are initiated, is less than this height lost value, the glider would impact the ground before reestablishing level flight. In essence, this plot shows the AAA envelope where recovery using the conditions indicated would be successful. The second contour plot shows the airspeed at the time level flight is reestablished. In most cases or interest, this airspeed will be well in excess of that needed for level flight (at the assumed AoA) as it will occur at the bottom of the pullout. The third contour plot shows the maximum Gs the glider would incur during the recovery. This is essentially the greatest lift generated by the wing and, since the AoA is constant, would occur at the highest airspeed which, as just noted, generally occurs at the bottom of the pullout.

Without further adieu, the contour plot for the height lost is shown below. The height loss contours are at intervals of 25 feet.

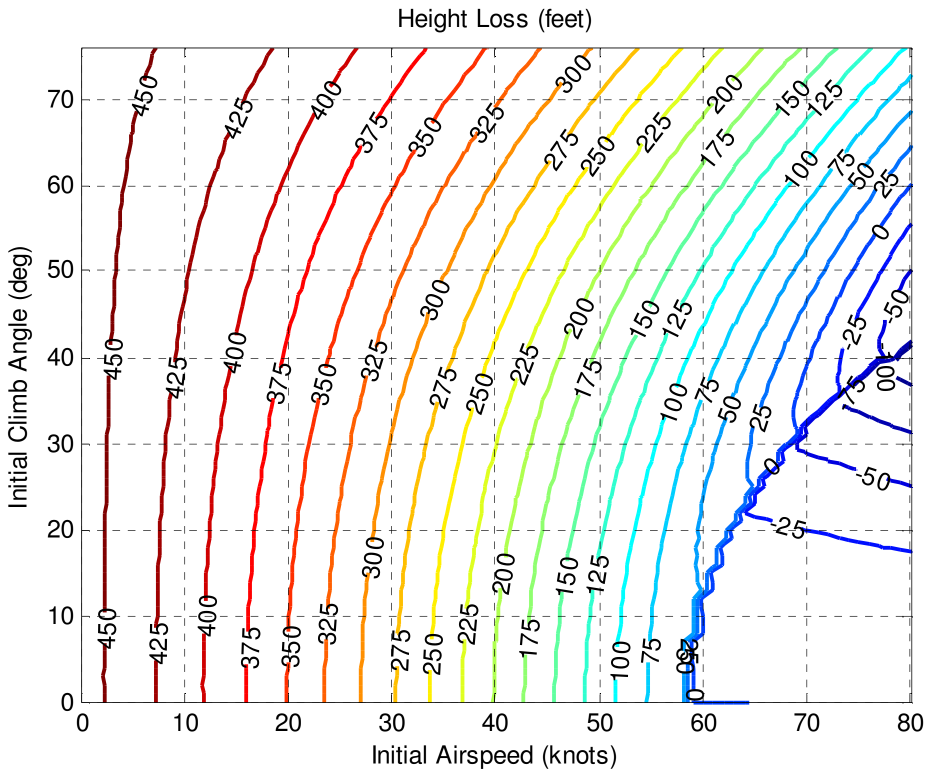

Figure 3. Height Loss for Recovery at 1.5 V_s AoA. V_s = 39 knots. *L/D* = 20:1.

Relating this to the trajectory plot above, those trajectories correspond to the 45° initial climb angle horizontal line. Note that, at 0 initial airspeed, the contours indicate the height loss is just over 450 feet. Reference to Figure 2 indicates the actual height loss is about 460 feet. A little above 70 knots (still along the 45° line), the height loss goes negative signifying the glider recovers having always remained above the height at which recovery was initiated. Other trajectory traces can be compared to this contour plot along the 45° line to see the mapping.

The upper left hand region is where one really doesn't want to be starting to initiate recovery. This is where there is little airspeed and a very steep climb angle. In reality, it is hard to imagine how any competent pilot could get in this condition before initiating recovery. It is actually difficult to get the glider well into this region while on the wire. So hopefully, left of the 40 knot vertical line is not an area we would expect a competent, aware pilot to be in. Furthermore, being at a high climb angle (attitude) without a large stall margin, meaning airspeeds in excess of 1.5 V_s (here over 58 knots), should be obviously undesirable. Unless the pilot is distracted and/or a very insidious power failure has occurred, being at angles above 45° with less than 55 knots is hard to explain. What this means is that it should generally be considered a major pilot error for the pilot to be in these regions of the plot at all. If we look at the contours of height loss at this 45°/55 knot point, we see that the expected height loss upon initiation of recovery is between 125 and 150 feet. So we can see that it would be unwise to be at less than 150 feet and 55 knots as the climb angle approaches 45°. But if the airspeed at 45° is 70 knots, less than 25 feet is required to recover. Starting at about 58 knots (1.5 V_s) and zero climb angle, a zero height loss contour begins and arcs up and to the right. This contour represents the airspeed/attitude combinations where a zero-G pushover to level would result in the glider recovering with no height loss whatsoever from the point of initiation. [The somewhat ragged behavior along this line is due to the very close solutions where the recovery is complete at the top of the pushover or where a short dive/pullout is needed.]

Unless very low tensions and/or excessive rotation rates are being employed, it is hard for the glider to reach a very significant climb angle before sufficient altitude is available for recovery. For example, if the initial rotation rate is 10°/s and a 0.5 tension factor is being employed, the airspeed is increasing about 9.5 knots/s early in the rotation. If liftoff begins at 50 knots, by the time the glider has reached 10° climb angle a second later, the airspeed is approaching 60 knots. 60 knots and 10° can be recovered from with no altitude loss so any altitude gained during this time becomes additional margin. Once the airspeed has reached 70 knots, the climb angle has to exceed 40° before any altitude need be lost once recovery is initiated. But this airspeed would be reached a little over 2 seconds at this rotation rate so the attitude would only be a bit above 20° at this time. What is seen is that, with reasonable rotation rates and tensions, the glider stays well within the recoverable AAA envelope.

For moderate airspeeds, the climb angle at the initiation of recovery is a relatively second order effect, i.e. the contours are close to vertical. At the higher airspeeds and attitudes, the effect is more pronounced but we are generally talking about recoveries where there is little altitude loss involved or an actual gain occurs during the recovery. An important point here is that maintaining appropriate airspeeds throughout the rotation is fundamental to safe operation. The old piloting adage, “Speed is money in your pocket and altitude is money in the bank” is clearly evident here. What is exceedingly clear is that you want to have money in your pocket (airspeed) early in the launch. Modern certification requirements require V_w be at least 150 kph (81 knots). It is seen that for these assumptions over a 60° climb trajectory is required before any height need be lost at all at this airspeed.

The takeaway from all of this is that a competent, attentive pilot using anywhere near reasonable rotation rates and maintaining appropriate airspeeds can always be in a readily recoverable condition regardless of any plausible peak climb angles. With adequate airspeed, high climb angles are not intrinsically dangerous and recovery should not be difficult to if proper actions are initiated promptly and effectively. Again the key words here are promptly and effectively. Training and awareness are key to safe operation.

An interesting aside is a question that has occurred to me in the past. If I were pushed off a vertical cliff, how high would the cliff need to be for me to attain level flight before impacting the ground? Looking at the 0 airspeed line, the height required is about 460 feet. This is likely higher than many pilots might think. While not associated with winch launching, this is relevant to a pilot who has pulled the glider up to vertical and let the airspeed decay to near zero. Executing a hammerhead or whip stall is close to this condition and this is the amount of altitude that might be expected to be lost during the recovery.

The second contour plot below shows the peak airspeed during the recovery. The contour interval here is 5 knots.

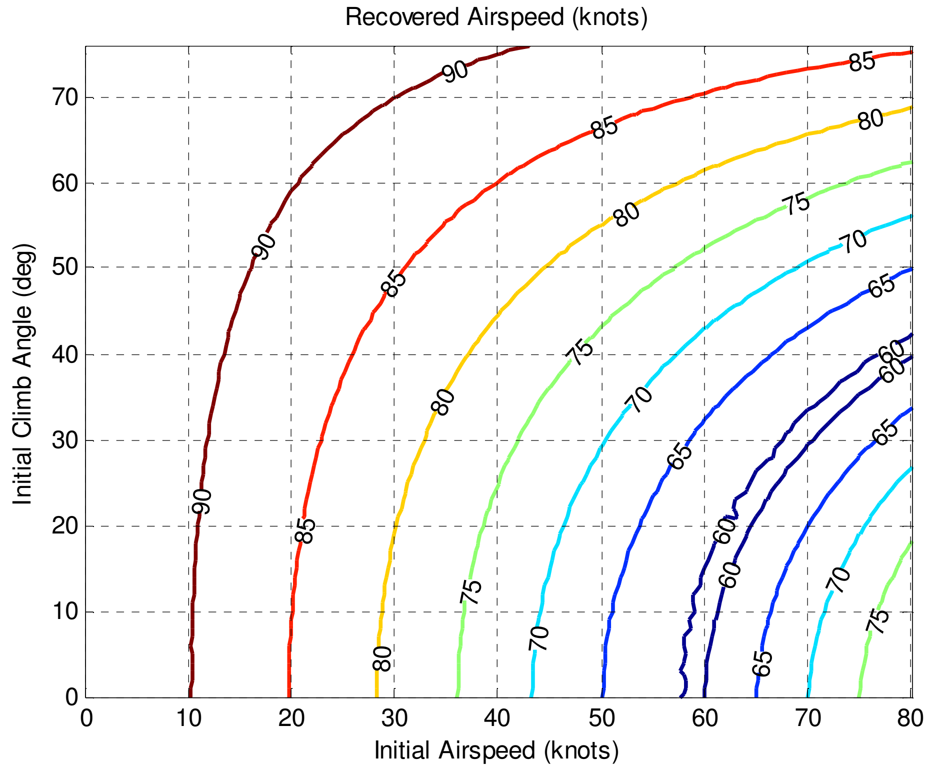

Figure 4. Peak Recovery Airspeed at 1.5 V_s AoA, V_s = 39 knots, L/D = 20:1.

As can be seen, initiating the recovery at lower airspeeds and higher attitudes results in higher peak airspeeds during the recovery. In the region where the pilot should be initiating recovery, the airspeed need never exceed 80 knots. This is below maneuvering speed for most gliders so overstressing the aircraft should not be an issue. However, stalling the aircraft during recovery is always possible and is always an issue. Regarding the hypothetical glider off a cliff scenario, the airspeed here can approach 100 knots. Similar airspeeds could be expected recovering from a hammerhead or whip stall.

Of note is that the airspeed at recovery reaches a minimum of about 58 knots and then begins increasing again. What is happening to the right of this minimum is the recovery is actually complete at the top of the ballistic arc, i.e. the glider is level and at or above the airspeed, 1.5 V_s, required to sustain unaccelerated (slowly descending) flight at that AoA. The contours then represent the airspeeds at the top of the ballistic arc which are lower than the initial airspeed, i.e. some airspeed has been converted to height.

The final plot indicates the maximum Gs pulled during the recovery. The contour interval here is 0.2 Gs.

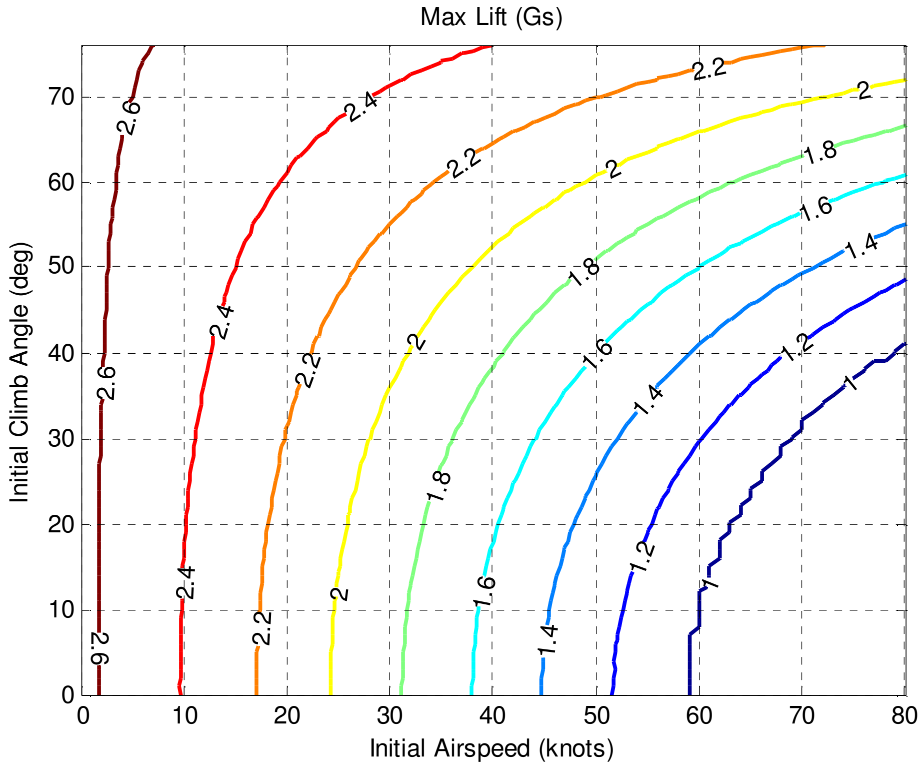

Figure 5. Maximum Gs at 1.5 V_s AoA, V_s = 38.9 knots, *L/D* = 20:1.

When recovery is initiated in the prudent region, the maximum Gs needed during the recovery should be well under 2 Gs. The stresses on the airframe and pilot are minimal here, well under that for a coordinated 60° banked turn. Note however the extreme left hand portion of the plot where the G loads are over 2.6 Gs. Finally, the 1 G plateau in the lower right corner is where the recovery is complete at the top of the ballistic arc.

With the presentation and interpretation of these preliminary results completed, some opportunities for safely operating beyond the current recommendations are identified. Then further elaboration on the models employed is presented. These elaborations may be skipped for those less interested. After this development variations on these simulations are considered. These include recovery at different AoAs, different stall speeds, the effect of drag (actually no drag) on the recovery, use of negative G pushovers, and the effects of density altitude. The effects of each of these variations are explored by comparison with the above reference results. Most of the serious mathematical developments are deferred to the Appendix so as not to distract the interested reader from absorbing the effects of these variations. The net conclusion is the preceding reference results are generally very conservative and there are opportunities to further expand the recoverable AAA envelope particularly if the glider is equipped with an AoA instrument.

Advanced Operational Opportunities

BGA recommendations call for rotation rates of no more than 10°/s. From the above, it is clear that this will generally result in the glider being in a recoverable condition so long as the airspeed remains sufficiently high. To my knowledge, there are no gliders with rate of rotation indicators so this is not directly actionable guidance. No pilot can precisely control the rotation rate. What this really goes to is that a rotation to a climb angle in the mid 40's should take about 4 to 5 seconds and be reasonably smooth, i.e. more an average rotation rate. After some height and appropriate airspeed has been established, momentarily exceeding this average rate is not problematic. In general, I support these BGA recommendations for classic winches launching gliders without an AoA indicator.

However, the above results, and the results to follow, indicate that rotation rates in excess of this value can be safely used during the rotation. This would be enabled through the availability of tension controlled winches and AoA indicators in the glider. The primary value of such techniques is for operations with limited cable runs where there is value in maximizing the launch height to make winch operations at the site feasible. But, the incremental benefits of such methods diminish rapidly with increasing run lengths. There is little motivation to use such techniques for longer runs (> 1000 m) and increased safety margins result from employing more conservative rotations. As there are no accurate tension controlled winches available today and very few gliders have AoA indicators, such methods are not generally prudent to employ at this time. When such equipment is available, a reasonable operating paradigm would be to lift off when above approximately 1.3 V_s and slowly begin to rotate as the airspeed builds, i.e. a short safety climb. The rotation rate can be smoothly increasing during this safety climb. As the airspeed passes through 1.5 V_s the rotation rate can begin to exceed 10°/s. By the time the airspeed has reached 1.8 V_s, the rotation rate could very safely be on the order of 15°/s (or even higher). As the climb *angle* exceeds 45°, the rotation rate should begin to be tapered back as the lift required increases rapidly above this angle for high rotation rates. The rotation rate should be smoothly tapering down towards zero. The airspeed should be continually rising to and through the target climb airspeed but should not peak above V_w (although there is some merit to letting it even exceed this value momentarily). As the final climb angle is approached, determined by the climb tension, the rotation rate should reach zero unless the airspeed is above the target climb airspeed (recommended) in which case the climb angle can increase momentarily above this peak climb angle to pull the airspeed back to the target. This implies a short negative rotation rate period where the climb angle falls back to that required to hold the target climb airspeed. The technical justification that such rotation rates can be safely employed can found in [1]. The key to safely employing this method is monitoring the airspeed and AoA throughout the rotation. Here monitoring the AoA is to further insure that the glider does not get anywhere close to stall AoA due to the lift required to counter the combination of centripetal, gravity, and cable forces. A tension controlled winch minimizes the probability of a cable/weak link failure during the launch by accurately controlling the cable tension throughout. (Note that this is not constant tension during the rotation.) The glider/pilot dependent rate of tension ramping employed naturally leads the pilot to use such rotation rates to contain his airspeed. Lower tension ramping rates drives more conservative rotation rates. Insuring that adequate airspeed is maintained throughout the rotation so that the glider remains safely in the AAA envelope is the final piece of the puzzle. Properly implemented, should a launch failure occur, the glider can always be well inside the AAA envelope for safe recovery and the AoA can facilitate precise execution of the recovery maneuver. Again these advanced methods are not suggested for use with classic winches, for gliders not equipped with an AoA indicator, or for inexperienced pilots that do not understand the complex dynamics of the rotation or proper recovery execution. These are simply identified as opportunities that could be safely brought to practice with appropriate equipment and training.

Constant AoA Recovery Model Development

With the basic premise of the ballistic pushover and constant AoA recovery strategy established, the theoretical development of how such recoveries may be simulated are now developed and interpretation of the resulting trajectories is provided. Since the assumption is that this predetermined AoA is established near the pushover peak and is held throughout the pullout, first consider what happens for different airspeeds with different AoAs starting at the peak. To begin, a lossless model is developed with drag effects included later.

Basic aerodynamics theory states that lift is given by

$$L = \frac{1}{2}\rho V^2 S\, C_L$$

where L is the lift, ρ is the air density, V is the true airspeed, S is the wing area, and C_L is the coefficient of lift. The coefficient of lift is determined by the angle of attack and increases approximately linearly with AoA (relative to the zero lift axis) until stall is approached. C_L is maximum near stall and then falls or plateaus with further increases in AoA. The induced drag level increases rapidly as this critical AoA is approached. Some define the stall AoA as the angle associated with maximum C_L. But fundamentally, C_L is determined by the angle of attack and fixing the angle of attack essentially fixes the coefficient of lift. The model employed simplifies this relation to its essence which is

$$L = \lambda V^2$$

i.e., the lift generated is proportional to the airspeed squared when the AoA is held constant. All the other terms are collected in λ, the constant of proportionality. Later in the paper, the effects of density altitude are considered but for now the analysis will assume standard sea level conditions.

With this relation, a relatively simple set of non-linear (because of the squared airspeed term) $F = M\,A$ differential equations may be developed as described in the Appendix. The solution of these equations for different initial conditions and values of λ provide insight into the recovery process.

Determining λ from the angle of attack would be a formidable task but a simpler approach that can be readily related to some basic glider performance parameters is employed as outlined earlier. Stall speed is the minimum airspeed where the wings can sustain the weight of the glider i.e., the minimum speed where the lift L is equal to the glider weight. Operation at this speed implies the glider is operating near the maximum C_L AoA. Normalized to the glider weight, this is termed a lift factor or 1 or 1 G wing loading. But if the glider is operated in level flight at a higher speed, the lift factor is still 1 so the C_L and AoA are both lower resulting in a lower value for λ. In the mathematical model, what is important is the lift factor – the glider mass falls out of the equations. The way the angle of attack will be characterized is with regard to the AoA that would yield a lift factor of 1 at a defined speed, $V_1 = k\,V_s$, relative to the stall speed. The lift factor, $L\,/\,MG$, simply becomes

$$\frac{L}{M\,G} = \left(\frac{V}{V_1}\right)^2 = \left(\frac{V}{k\,V_s}\right)^2$$

If the glider were equipped with an AoA meter, stall AoA would be clearly marked and the AoA for different values of V_1 could be ascertained by establishing stabilized level (again for now we are assuming lossless) flight at these values and noting the indicated AoA. Many gliders achieve minimum sink around 1.3 V_s and best L/D at around 1.5 V_s so pilots can readily relate to these values. The actual angle of attack itself is not important for this development.

It should be noted that a constant stick position may not result in a constant AoA recovery. Most aircraft exhibit a pitch control force behavior referred to as stick force per G, i.e. the required stick force increases with the Gs being pulled. In a constant AoA pullout the Gs are increasing throughout so this force will be changing but how the stick position will vary throughout the constant AoA recovery is not obvious. Ideally, holding a constant AoA will not require much stick movement but the force to hold the stick in this approximately fixed position would likely increase through the recovery.

Lossless Constant AoA Pullout Simulations

Using this characterization of AoA, simulations of this model provide great insight into pullout behavior. For the baseline, we have assumed a representative glider with a stall speed of about 39 knots (20 m/s) and observe the trajectories that result with different airspeeds over the top for several AoAs characterized as described. Figure 6 illustrates these lossless flight trajectories for initial airspeeds between 0 and 55 knots for an AoA corresponding to V_1 equals 1.5 V_s or about 58 knots.

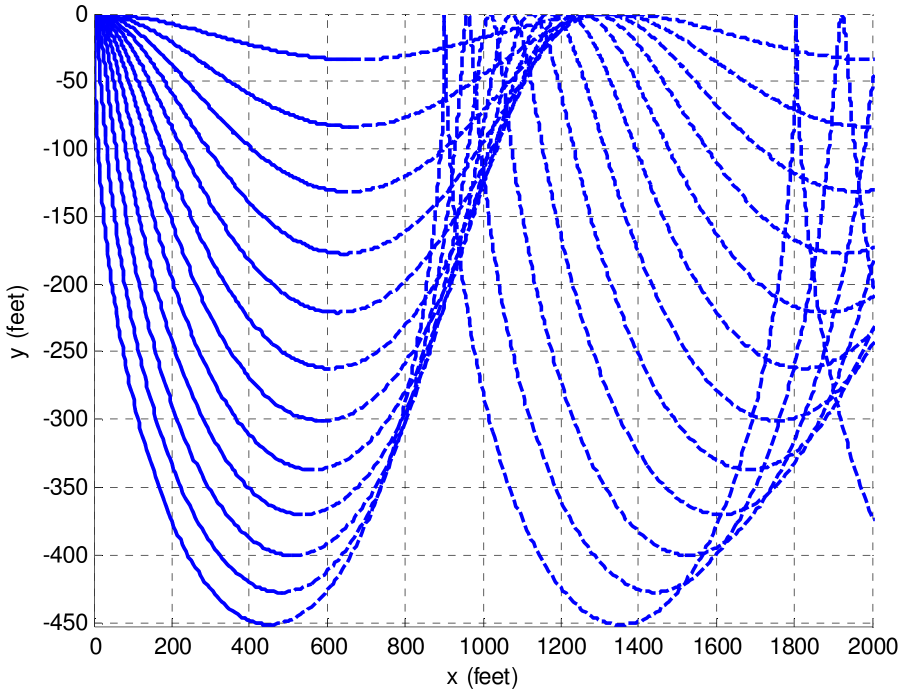

Figure 6. Lossless Constant AoA (1.5 V_s) Flight Trajectories

These trajectories should be very plausible to aviators under this lossless assumption. Normally we would only be interested in the trajectories until level flight returns at the bottom of the pullout as represented by the solid traces. However, the simulations were allowed to continue (the dashed traces) and a periodic behavior is observed where the glider climbs until it returns to the original height and speeds then repeats this cycle indefinitely. This is a characteristic of the lossless nature of the model and will be contrasted later when drag is included in the simulations. What is seen from these simulations is that the height loss (from the peak) is a strong function of the airspeed over the top. An interesting (but not typical) trajectory is the height loss from 0 knots – just over 450 feet. As noted earlier, this would relate to the amount of height required for a pullout if a glider was pushed off a cliff or starting from a whip stall and corresponds to a worst case condition. The slight difference in height from the reference results is due to the absence of drag losses.

Simulation airspeeds greater than 55 knots are not illustrated. Those in excess of 1.5 V_s would mean the lift at the assumed angle of attack would be greater than 1 and the glider would climb further, not descend, when this AoA is established. [Mathematically these initial conditions would result in trajectories where this is the bottom of similarly shaped trajectories.]

Even more illuminating is to look at various aspects of these trajectories vs. time as illustrated in Figure 7.

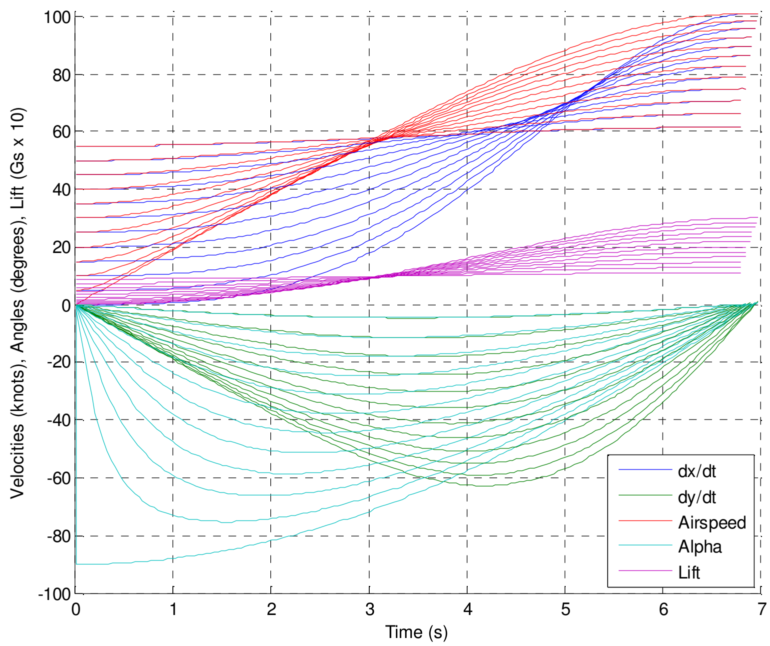

Figure 7. 1.5 V_s Pullout Simulations Results vs. Time

Shown are the vertical and horizontal velocities along with the airspeed (the square root of the sum of these components squared), the dive angles, and the lift factors (x 10 for scaling). Here the simulations are terminated at the bottom of the pullout. While these plots are very busy, some important aspects can be noted. These include for each initial velocity: the maximum airspeed (at the bottom of the pullout), the maximum dive angle, the maximum Gs being pulled (again at the bottom). Surprisingly, the dive times were all about 7 seconds. [This has suggested that there may be closed form solution for this Pullout Phase. Help from anyone proficient in non-linear differential equations would be appreciated.]

Initial Airspeed (knots)	Height Loss (feet)	Maximum Dive Angle (degrees)	Maximum Airspeed (knots)	Maximum Lift (Gs)
0	452	90	101	3.0
5	428	75	98	2.8
10	400	66	96	2.7
15	370	59	93	2.5
20	337	51	90	2.4
25	301	44	86	2.2
30	262	38	83	2.0
35	221	31	79	1.8
40	177	25	75	1.6
45	132	18	71	1.5
50	84	11	66	1.3
55	34	5	62	1.1

Table 1. Key Pullout Recovery Results for 1.5 V_s

The maximum pullout airspeeds range from 62 to 101 knots increasing as the recovery initiation airspeed decreases. The peak lift factors (Gs) are also maximum for the lowest airspeed over the top and peak near 3 Gs. The peak of 3 g's suggests that many pilots would not pull back sufficiently, i.e. tending to limit at lower G force, thus increasing the altitude lost. On the other hand a pilot seeing the ground coming up may pull back too hard before speed has increased. So, from these simulations, an immediate takeaway is that getting over the top with the maximum amount of airspeed results in the least height loss, excess airspeed, and Gs being pulled. Further discussion of this is deferred until the behavior with other AoAs is considered.

The previous simulation was at the angle of attack associated with level flight at 1.5 V_s. Figure 8, Figure 9, and Table 2 present simulation results for V_1 equals 1.3 V_s implying a higher AoA (and C_L). The initial airspeeds only go up to 50 knots due to V_1 being reduced to 50.5 knots. Here all the simulations are again terminated at the bottom of the pullout.

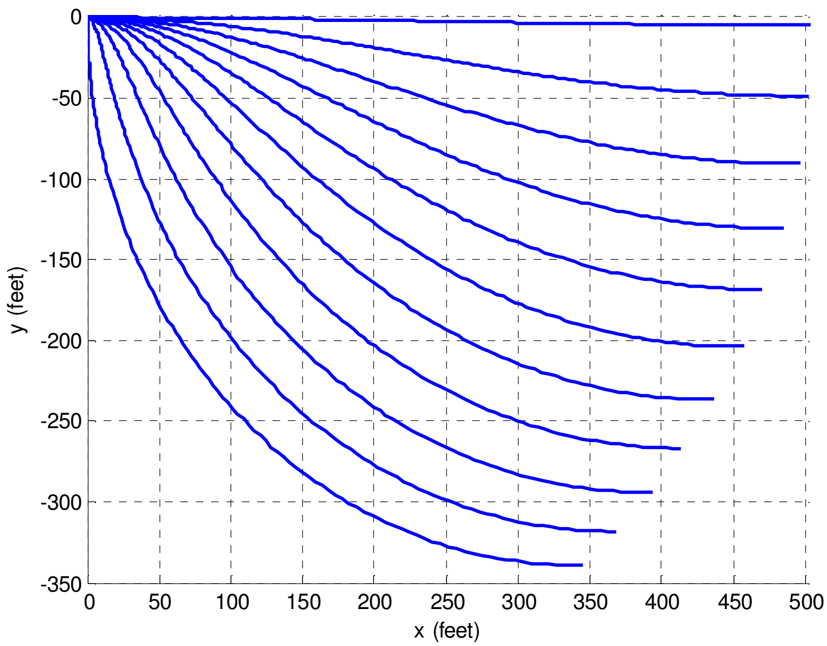

Figure 8. Lossless Pullout Trajectories for 1.3 V_s Associated AoA

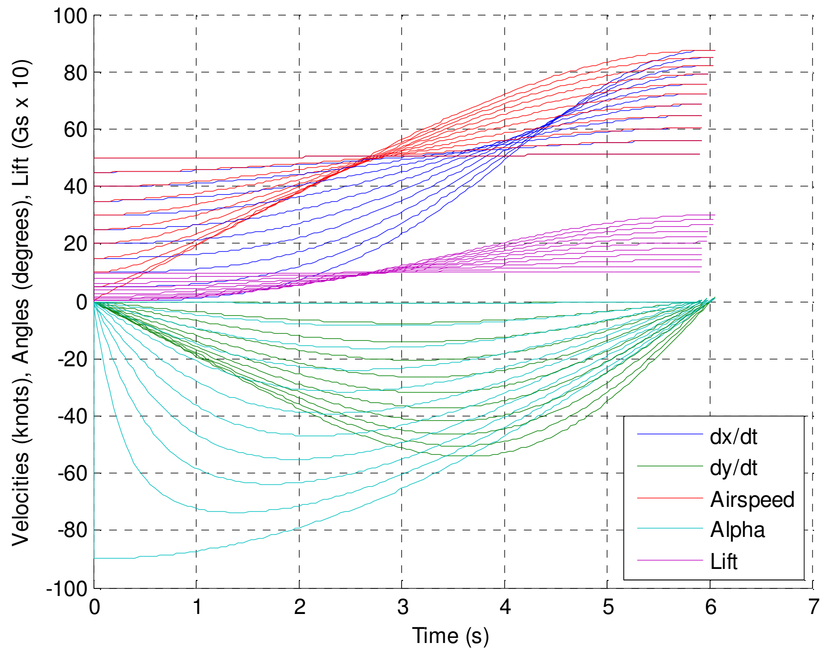

Figure 9. Temporal Pullout Responses for 1.3V_s

Initial Airspeed (knots)	Height Loss (feet)	Maximum Dive Angle (degrees)	Maximum Airspeed (knots)	Maximum Lift (Gs)
0	339	90	87	3.0
5	318	74	85	2.8
10	294	63	82	2.6
15	267	55	79	2.4
20	237	47	76	2.2
25	204	39	72	2.0
30	168	32	68	1.8
35	130	24	65	1.6
40	91	16	60	1.4
45	49	9	56	1.2
50	5	1	51	1.0

Table 2. Recovery Results for 1.3 V_s

When compared to the previous simulation set, it is seen is that the height loss and the excess airspeed are reduced substantially by using this higher AoA. The maximum Gs pulled are about the same for the zero airspeed case but are somewhat less for higher initial airspeeds. The time to recovery (about 6 seconds) is slightly reduced. Further simulations demonstrate that generally using a higher C_L yields an improved recovery. The greater lift at the lower airspeeds reduces the dive angle more quickly which reduces the height loss and airspeed buildup. Obviously the AoA employed must be less than the stall AoA (V_1 equals V_s) but, even before this angle is reached, the induced drag starts increasing rapidly. As will be discussed later in the paper, increased drag losses result in greater altitude loss during the recovery. There will be a point where these increasing drag losses outweigh the benefits of using higher AoA recoveries. But within limits, using higher AoAs generally yields superior recoveries with regard to height loss and exit airspeed. That this should be the case can be readily explained by recognizing that primarily there is a conversion of potential to kinetic energy during the pullout. If the recovery is higher, there is less conversion of potential to kinetic energy so the airspeed at the bottom must be lower. The downside to using higher AoAs for recovery is the reduced stall margin. Further discussion of the tradeoffs between lower height loss and stall risk is deferred until the Pushover Phase effects are included in the analysis, the next topic.

Pushover Inclusion

Given the angle and airspeed at the initiation of recovery and the assumption of a ballistic (zero lift) trajectory, the horizontal velocity component remains constant through this phase as gravity only affects the vertical component. At the top, the vertical airspeed component is 0 so the airspeed at the top (where the previous simulations began) is simply the horizontal velocity at the initiation of recovery. This velocity is simply given by

$$V_x = V_i \cos(\alpha_i)$$

V_i, the airspeed, and α_i, the trajectory angle, at initialization were previously defined with reference to Figure 1. Up to 45°, this horizontal airspeed component is at least 70% of the airspeed at the beginning of the recovery. Even for climb angles as great as 60°, the horizontal component is still 50% of the recovery initiation airspeed.

Simulations including the ballistic Pushover Phase are readily generated. It simply requires the lift be set to zero during the pushover (ballistic) portion in the simulation model. Simulations were run for the moderately high climb angle of 45° on initiation of recovery for initial airspeeds as before for V_1 equals 1.5 V_s and plots for these are presented in Figure 10 and Figure 11. The tabulated results are not presented as the contour depiction of the key results is used from here on. The initial airspeed now ranges up to 80 knots for 1.5 V_s and 70 knots for 1.3 V_s as there is some airspeed decay during the ballistic phase. The height losses are now referenced to the point the recovery pushover was begun, not the peak.

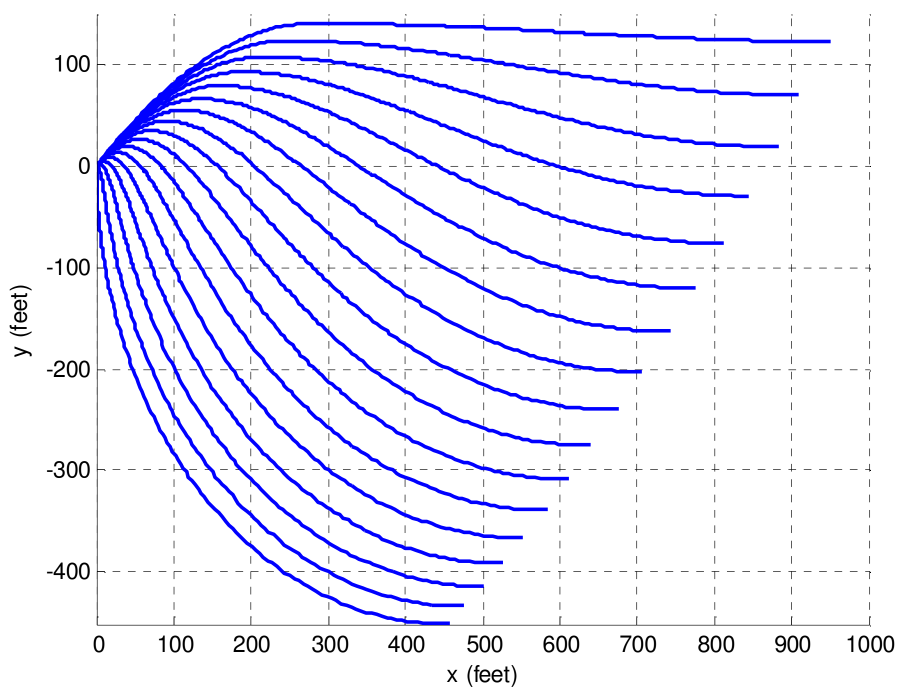

Figure 10. Lossless Recovery Trajectories for 1.5 V_s AoA. Initial Angle 45°, V_s = 38.9 knots.

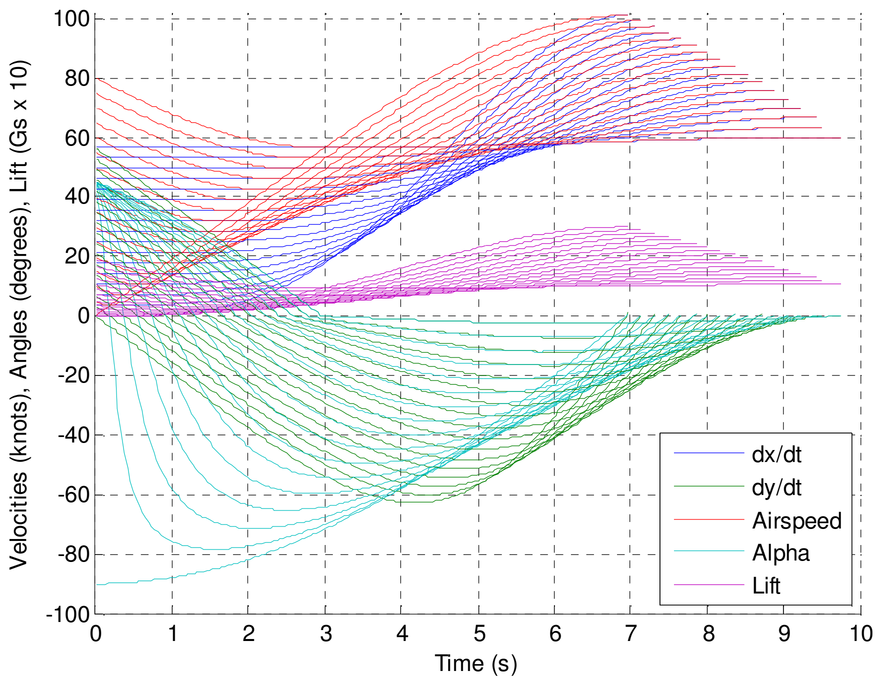

Figure 11. Temporal Pushover/Pullout Responses for 1.5V_s

What is new here is the height gain and duration of the Pushover Phase. Of note here is that the glider can recover near or above the launch failure height if sufficient airspeed is present at recovery initiation. It is unlikely that this initial climb angle would be established without some altitude being attained so that recoveries initiated at higher airspeeds can be very straightforward even from 45°.

Induced and Parasitic Drag Effects

Figure 12 illustrates the pullout trajectories when drag losses are included. Drag losses are simply included in the model as described in the development in the Appendix. Interestingly, both the parasitic and induced drags are proportional to the airspeed squared under the constant AoA assumption. These trajectories should be compared to those of Figure 6 where there were no losses. The *L/D* simulated here is 20:1 with the other parameters are the same as in Figure 6; AoA corresponding to 1.5 V_s with V_s 38.9 knots. The recovery again is initiated from a horizontal trajectory (0°).

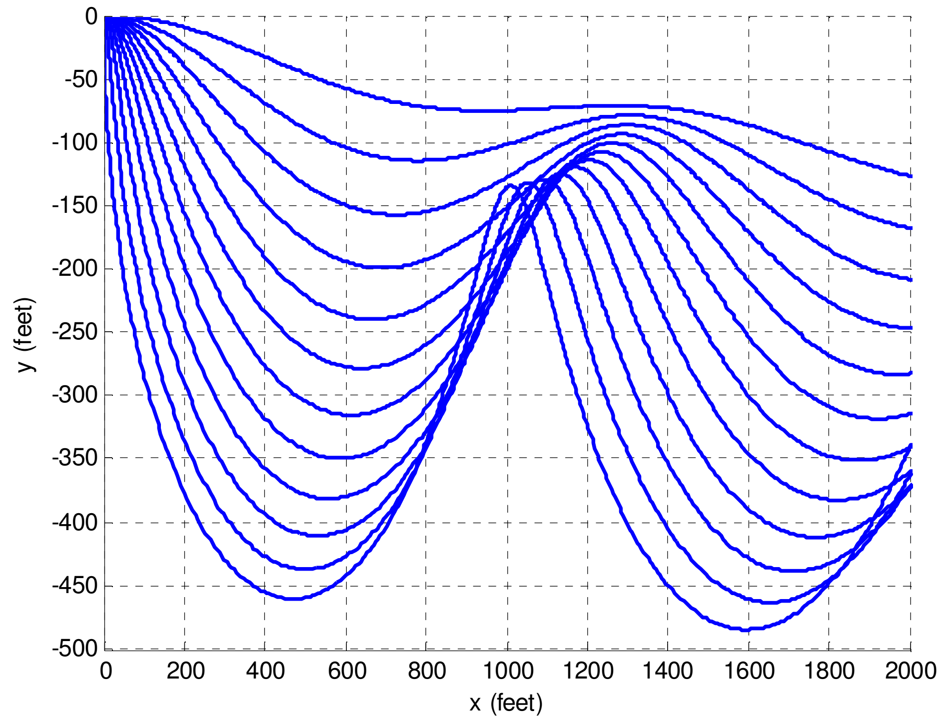

Figure 12. Reference Recovery Trajectories with Loss: *L/D* = 20.

The cyclic behavior is again observed but now the subsequent cycle peaks are successively lower representing the lost energy due to drag. The height losses for the first cycle vary from about 70 to 140 feet with the higher losses associated with the lower airspeeds over the top. This is not unreasonable as the lower airspeeds over the top result in higher peak pullout airspeeds and drag losses increase with the airspeed squared. If these trajectories are allowed to continue indefinitely, the amplitude of these cycles steadily decreases and asymptotically approach steadily descending flight at 58.3 knots (1.5 V_s) with a slope of 1/20 corresponding to the assumed 20:1 *L/D* at this AoA.

Many simulation plots could be run for climb angles other than the 0° and 45° used in these examples but absorbing all this information would be challenging. The contour maps of the height needed for recovery versus a two-dimensional surface representing the climb angles and airspeeds at the recovery initiation are the means employed to convey this information. These contour plots succinctly illustrate the recoverable AAA envelope for the scenarios depicted. The maximum airspeed attained and G forces are also similarly portrayed.

Figure 13, Figure 14, and Figure 15 depict the height loss, peak recovery airspeed, and maximum Gs contours for a lossless recovery with a 1.5 V_s AoA and 38.9 knot stall speed. The light (dashed) contours are the same as in reference Figures 3 – 5 where an *L/D* of 20:1 was assumed. The contour intervals have been doubled to 50 feet to keep the plots from becoming too cluttered.

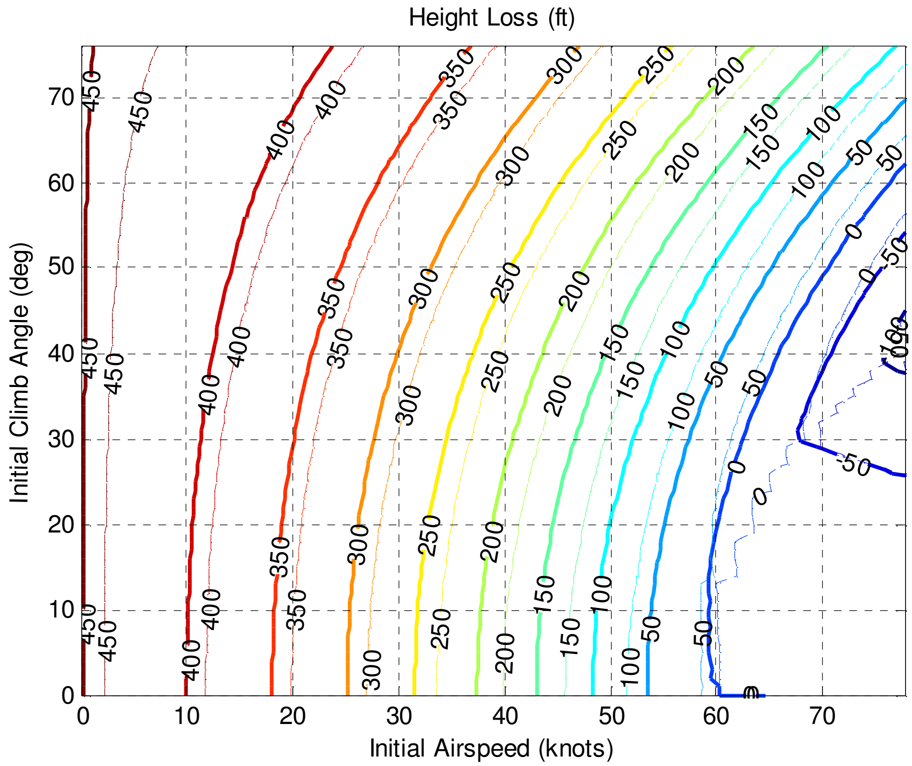

Figure 13. No Drag Height Loss for 1.5 V_s AoA, V_s = 38.9 knots.

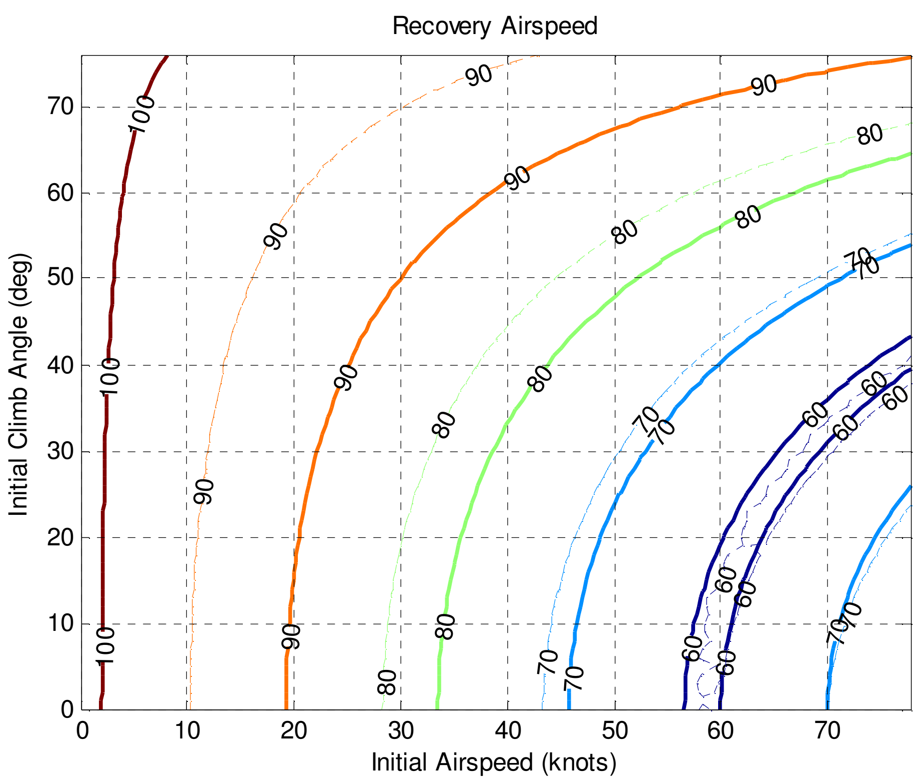

Figure 14. Lossless Peak Recovery Airspeed for 1.5 V_s, V_s = 38.9 knots.

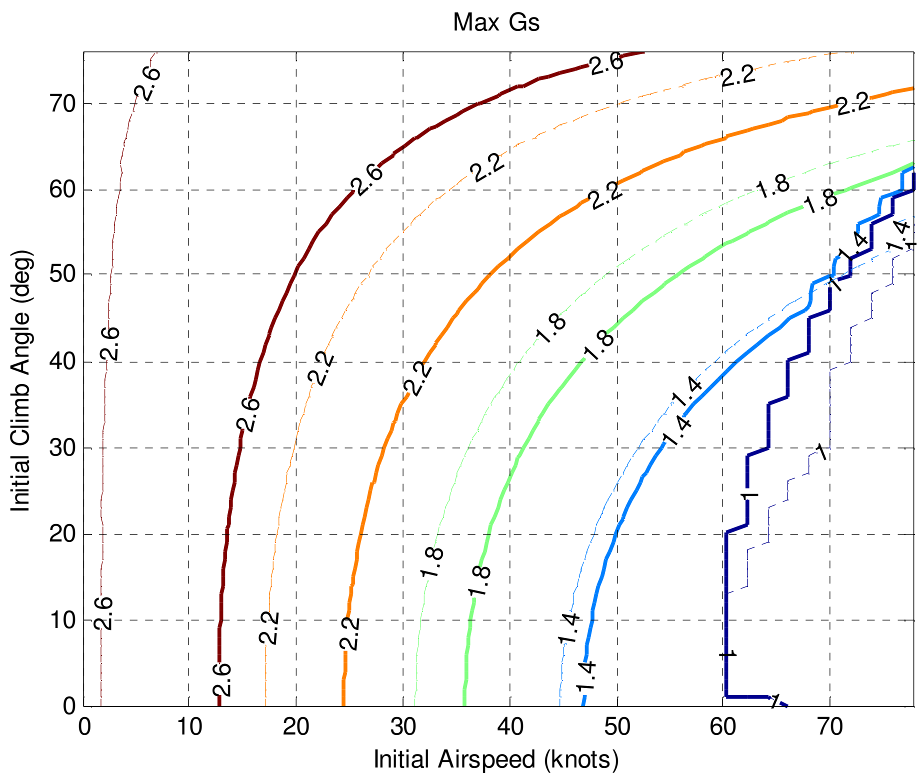

Figure 15. Peak Gs for Lossless 1.5 V_s AoA, V_s = 38.9 knots.

The height losses increase, but not significantly, when there are drag losses but the peak airspeed and G loads are noticeably decreased with drag losses. Apparently the drag reduces the rate of airspeed buildup during the dive/pullout. This reduced airspeed at the bottom naturally results in the reduced Gs at this point. The effects of drag are more pronounced at the lower airspeeds and higher climb angles but this is where we are hopefully not starting from in the first place. This is because the airspeeds at the end of the recovery are generally higher and this accentuates the drag effects.

It was noted earlier that the initial climb angle has a relatively small effect on height loss. Particularly at low initial airspeeds, the effect is minimal. More generally, this can be intuitively understood by the somewhat compensating actions of attitude and airspeed. If the airspeed is high, a high climb angle will result in significant height gain during the ballistic portion even though this high climb angle results in a lower horizontal airspeed velocity component which primarily determines the airspeed over the top. Again this all assumes a prompt and appropriate launch failure response.

Effects of Using Higher AoAs

We now consider the results for the higher AoA associated with 1.3 V_s. Figure 16, Figure 17, and Figure 18 present the height loss, peak airspeed, and peak Gs for this increased AoA.

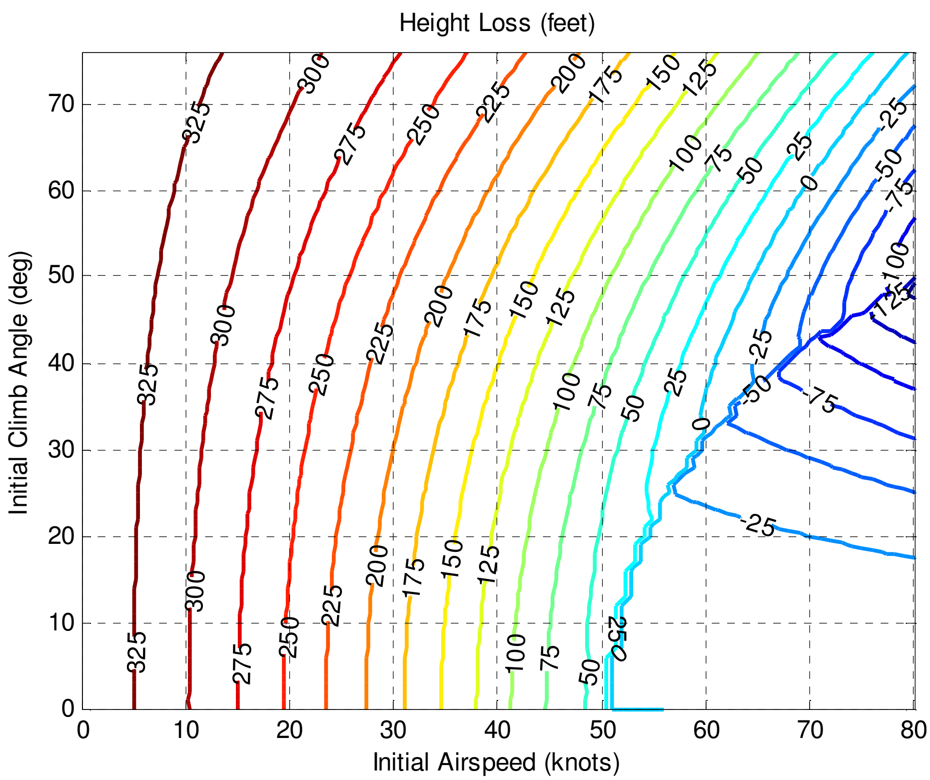

Figure 16. Height Loss at 1.3 V_s AoA, V_s = 38.9 knots, L/D = 20:1.

As suggested by the earlier pullout study, a benefit of using a higher AoA during the pullout is clearly evident as the height loss is reduced substantially in comparison to Figure 3. The "off-the-cliff" height loss has been reduced from over 450 feet to less than 350 feet. At the 45°/55 knot point, the height loss has been reduced to about 50 feet where before it was over 150 feet – a major reduction in a key area.

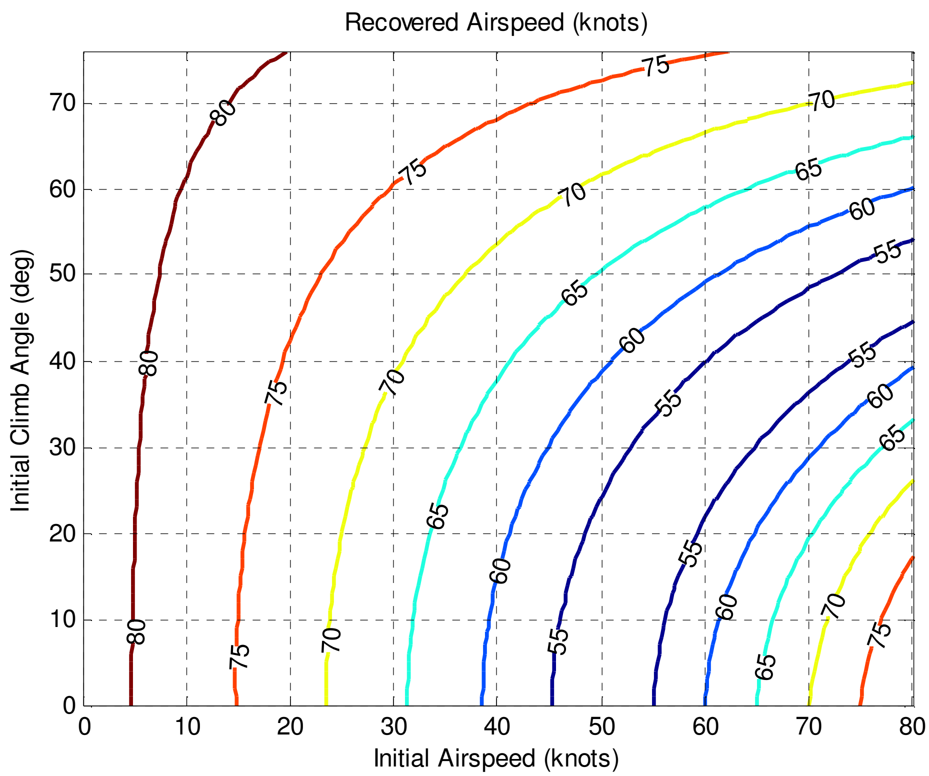

Figure 17. Peak Airspeed at 1.3 V_s AoA, V_s = 38.9 knots, L/D = 20:1.

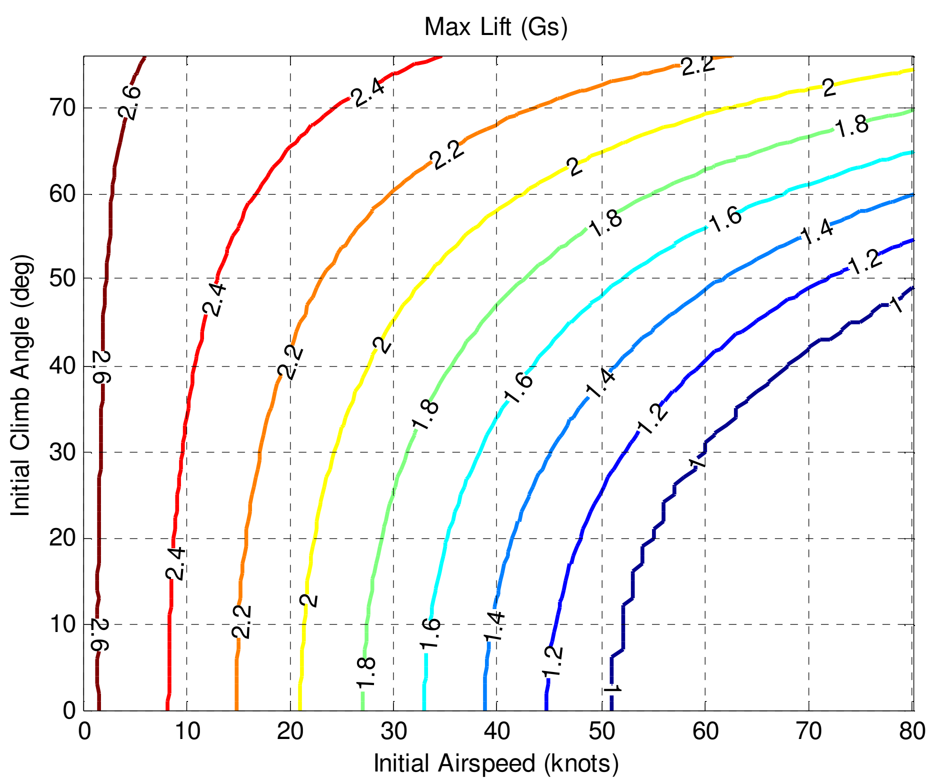

Figure 18. Maximum Gs at 1.3 V_s AoA, V_s = 38.9 knots, L/D = 20:1.

The peak airspeeds are also lower across the board. At the extreme left, less than 90 knots as compared to almost 100 knots before. The minimum well has dropped to about 50.4 knots (between the two 55 knot contours. Similarly, the peak G loads are also reduced somewhat. Not so much on the chart left side but more so in the region of interest.

The downside is the reduced stall margin present during the recovery. To perform this recovery method properly requires an AoA indicator, which is not common in most gliders. In general, pilots must choose how aggressively they recover and trade off reduced height loss with the increased risk of stall. If the failure occurs high, there is little motivation to use an aggressive recovery. The higher G loads with a lower AoA pullout are nowhere near any dangerous limits and any excess airspeed at the bottom can be mostly converted back to height. However, if the height available is marginal, use of a more aggressive pullout may be the only option but judging this under the high stress of a low launch failure is exceedingly problematic.

Effects of Increased Wing Loading (increased stall speed)

Next the effect of stall speed is explored. The scenario here employs the reference 1.5 V_s AoA but assumes a high wing-loaded glider such as a fully ballasted glider. The stall speed here is assumed to be 25 m/s, about 48.6 knots. The height loss and peak recovery airspeeds are shown in Figure 19 and Figure 20 respectively. There is little change in the G loads so these are not included.

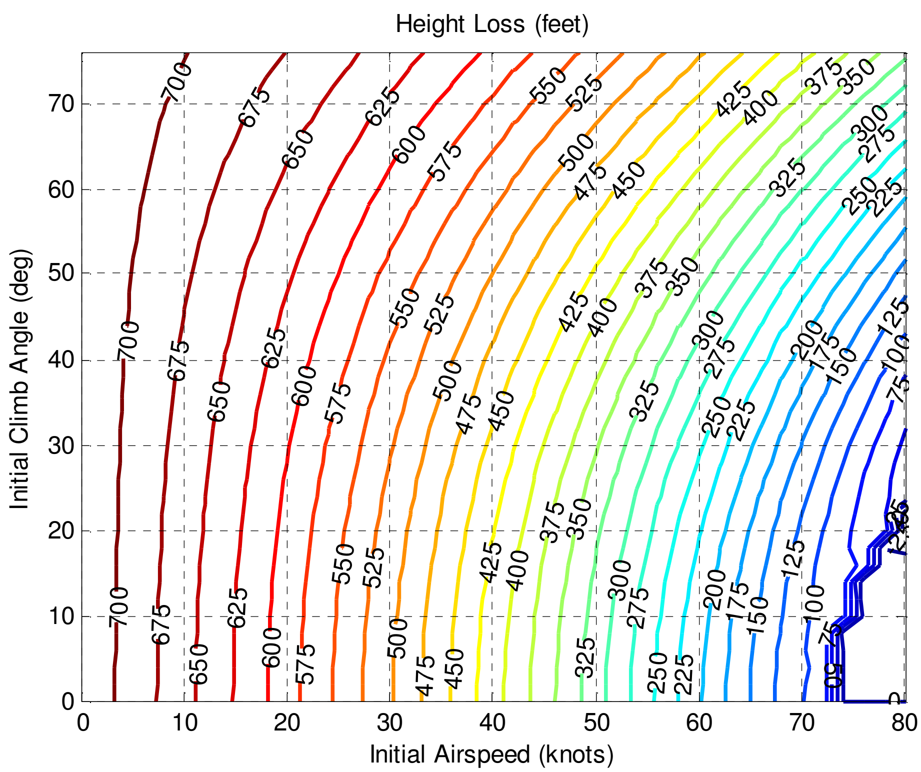

Figure 19. Height Lost at 1.5 V_s AoA, V_s = 48.6 knots. L/D = 20:1

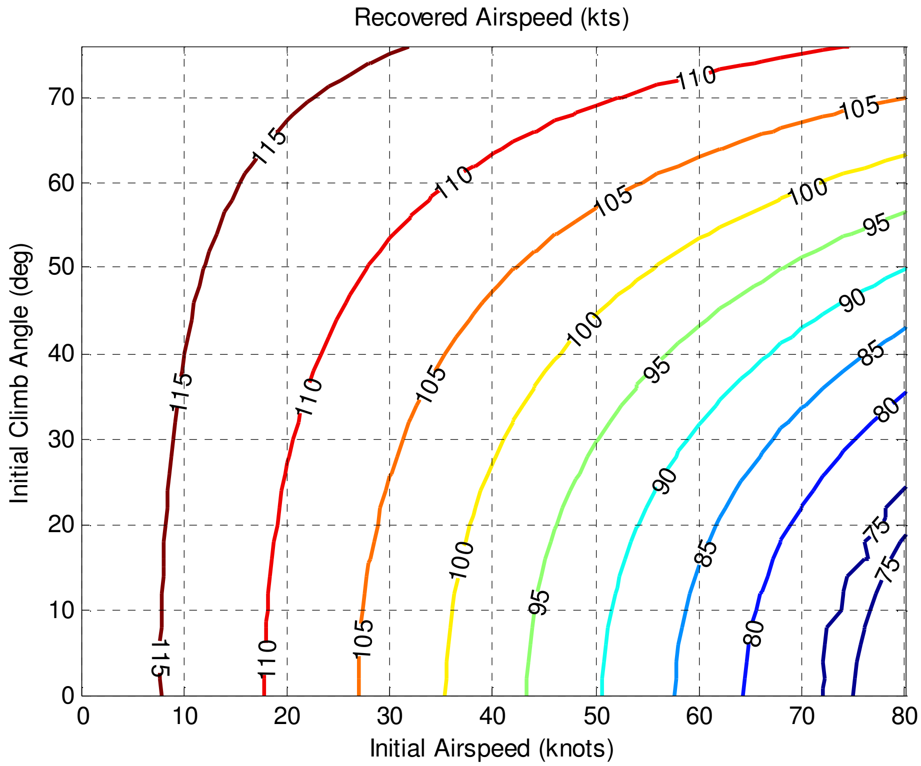

Figure 20. Peak Recovery Airspeeds at 1.5 V_s AoA, V_s = 48.6 knots, *L/D* = 20:1.

Both the height loss and the peak recovery airspeed are considerably higher – the "off the cliff" scenario is now over 700 feet now with airspeeds approaching 120 knots. The zero height loss contour now begins at almost 75 knots. Further studies have indicated that the height loss approximately increases with the square of the stall speed for 0 initial airspeed. No such generalizations can be made for other initial airspeed/attitude combinations other than the height loss and recovery airspeeds increase rapidly with higher stall speeds. Obviously, much greater care should be exercised when launching gliders with higher stall speeds (wing loadings).

Alternate Pushover Strategies

So far in the discussion the pushover has been assumed to be performed at 0 Gs, essentially where there is no lift being produced by the wing. Parasitic drag has been included but it is not a major factor. This is widely held to be the appropriate strategy. That this is a good strategy is now demonstrated and a superior strategy is then identified.

The question could be asked, why not hold the fixed AoA throughout the pushover and the pullout? It could be argued that holding this AoA throughout the upward arc would result in a higher altitude at the peak due to the lift generated through this period and the wing could still not stall. Figure 21, Figure 22, and Figure 23 are the height loss, peak recovery airspeed, and maximum G loading associated with holding the AoA fixed throughout the recovery. The solid contours are with constant AoA throughout the recovery and the dashed ones are the reference results using a zero-G pushover. The contour intervals are again increased to reduce clutter. The AoA is that associated with 1.5 V_s and the stall speed is 38.9 knots in both.

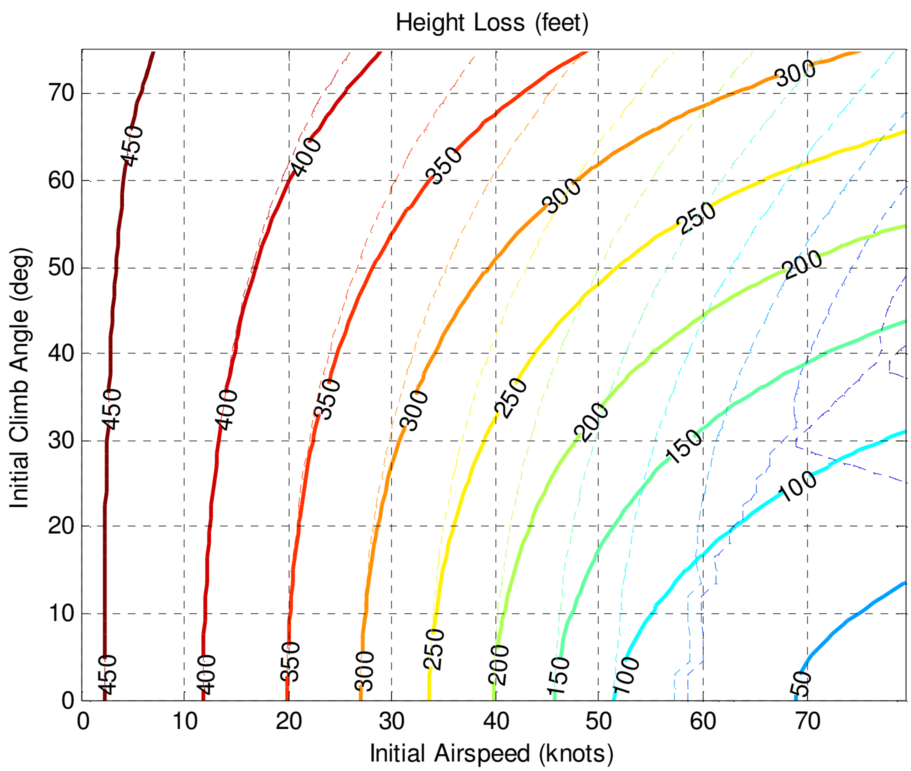

Figure 21. Height Loss with Constant AoA Pushover/Pullout

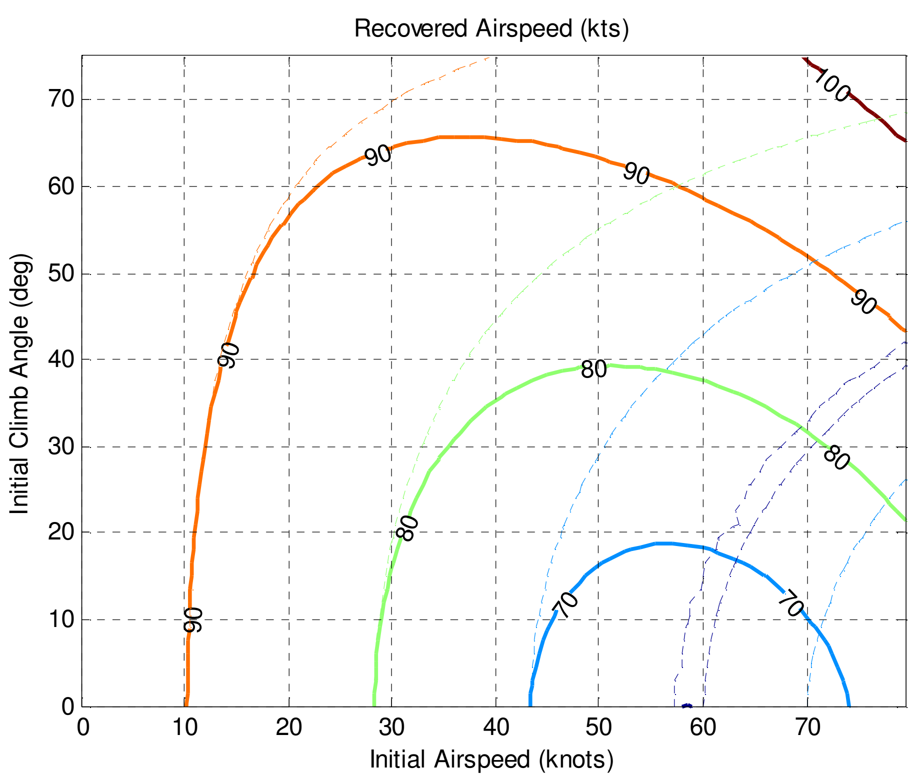

Figure 22. Peak Airspeed for Constant AoA Pushover/Pullout

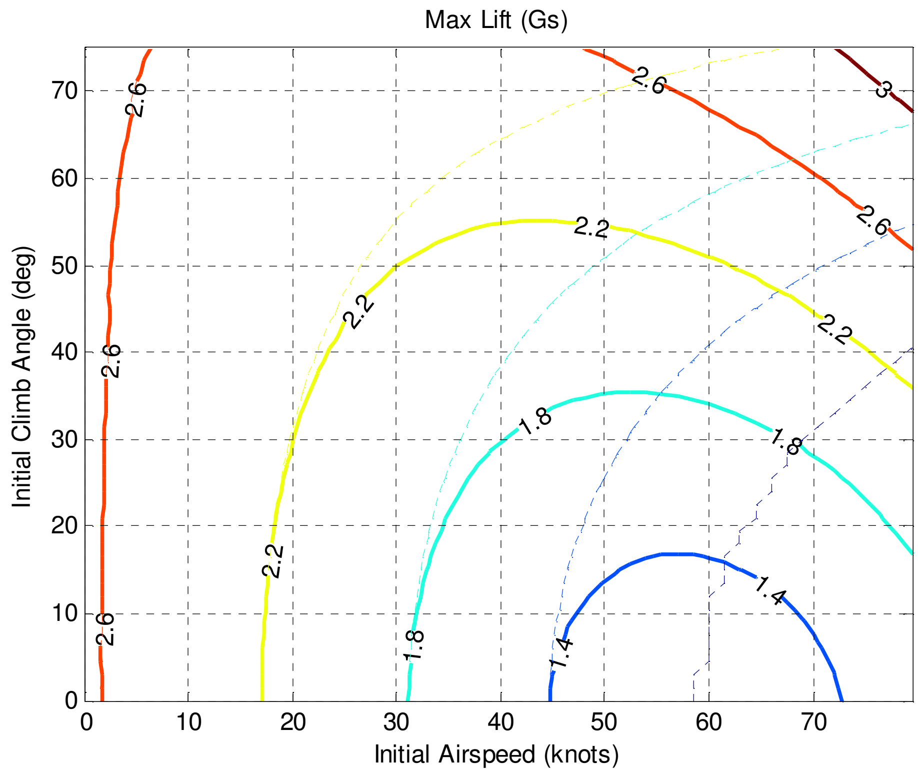

Figure 23. Peak Gs for Constant AoA Pushover/Pullout.

What is seen is the solutions for a 0° climb angle are the same with either technique. But this is simply because at 0° the recovery is effectively starting at the top and there is no Pushover Phase. Similarly, the responses do not differ much at the lower airspeeds regardless of the climb angle. But again this is easily explained as, with little airspeed, there is little pushover period before the trajectory peaks. Where the results differ most is for the higher airspeeds and angles. What is seen is that for, airspeeds above 40 knots and trajectory angles above 30°, the height loss is considerably greater using this technique. Similarly, the peak airspeeds and G loads both increase considerably in this region of most interest. This reinforces the earlier conclusion that getting over the top with as much airspeed as possible yields better recoveries. While the top may be higher, the airspeed there is lower and that more than counters any benefit of peaking out at a higher altitude. The behavior in the extreme right of the plot becomes more complicated to explain. Interpretation of the behaviors in this region will not be developed here as the negative aspects of this scheme should be clearly evident in the region of prime interest.

Negative-G Pushover

What about going the other way – using some negative Gs during the pushover? This corresponds to using a negative AoA during this period. Most modern non-aerobatic wings do not operate well at negative AoAs. Instead of assuming the negative lift has the same coefficient of lift as during the pullout, the simulations now presented assume the C_L magnitude is one-half that associated with the pullout. The induced drag would generally increase but, for these simulations the same parasitic drag factor is employed as for the zero-G pushover. Figure 24, Figure 25, and Figure 26 illustrate the height loss, peak airspeed, and peak Gs respectively for this negative AoA pushover. The heavy solid contours are for negative G pushovers and the light dashed traces are the reference results as always.

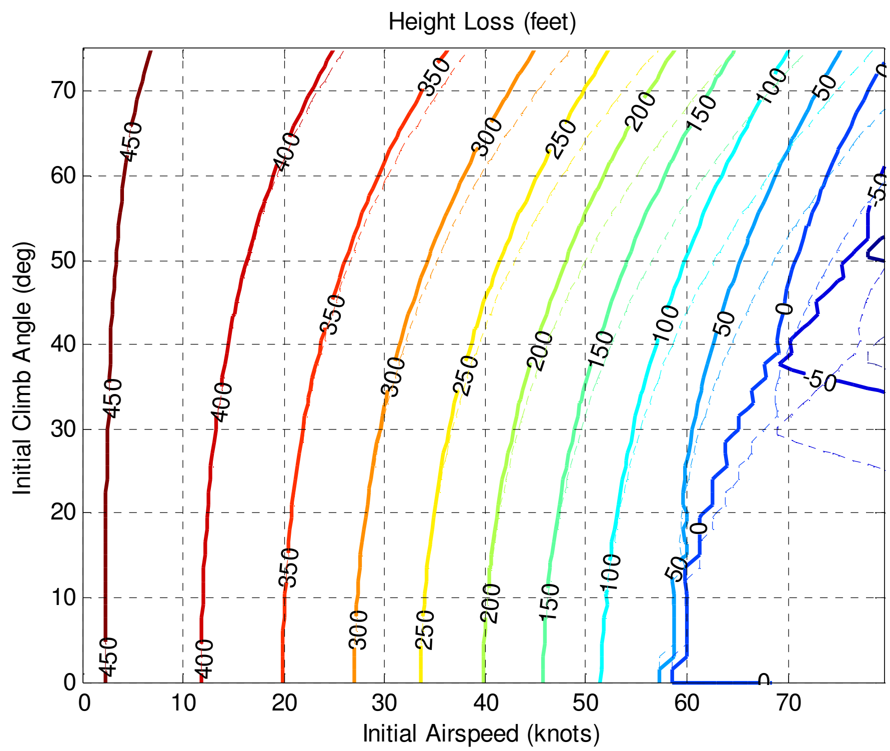

Figure 24. Height Loss for Negative AoA Pushover.

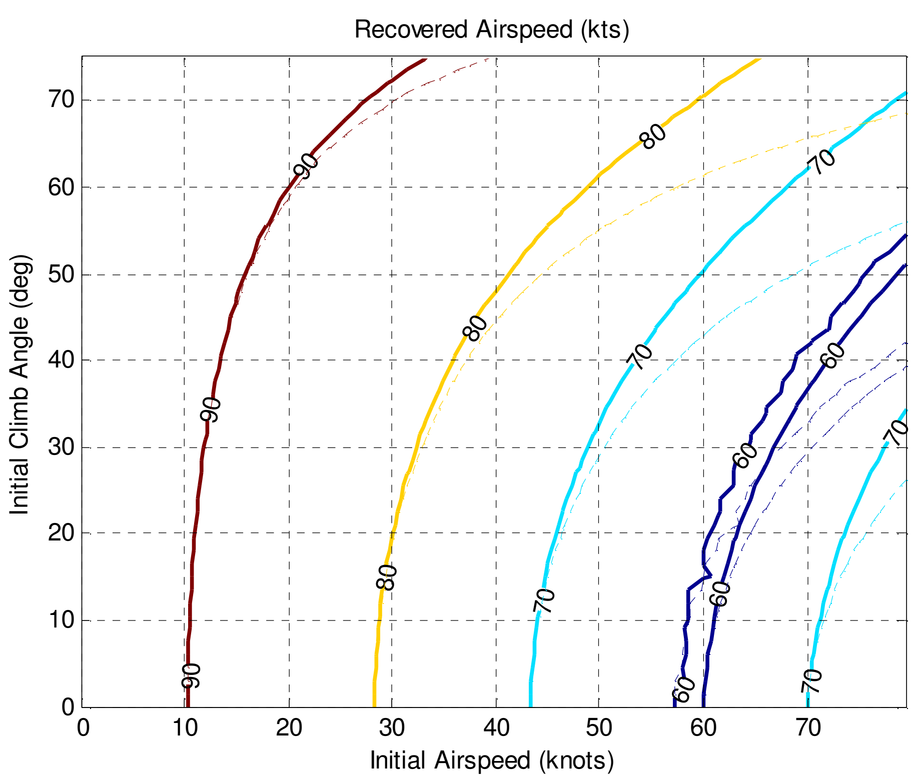

Figure 25. Peak Airspeed for Negative AoA Pushover.

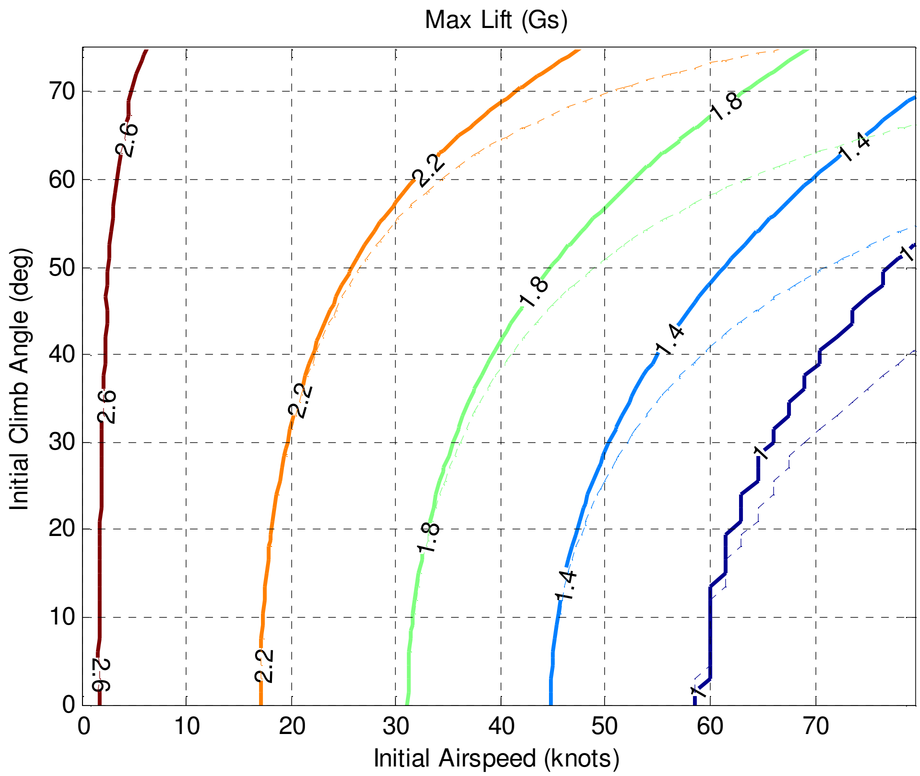

Figure 26. Peak Gs for Negative AoA Pushover.

What is clearly evident is these recovery metrics are actually improved using this technique – particularly in the regions of most interest. The contours become more vertical signifying the recovery is even less dependent on the climb angle at the time recovery is initiated. While the peak height is reduced, the airspeed over the top is increased and this is again seen to be the key to improved recoveries. The improvements are most dramatic for higher initial airspeeds and climb trajectory angles as these makes the Pushover Phase a larger part of the recovery. It is when the climb angle is high that the pilot would naturally want to get the ship over the top quickly and this is precisely when using some negative Gs is most valuable. The downside of this scheme is the possibility of a negative AoA stall. If this should happen asymmetrically, a spin could result. The risk of stalling increases with lower airspeeds. But the lesson here is clear, getting the glider ballistic or even a bit negative immediately is key to the recovery. Just as we teach new pilots to get the nose down quickly on a low level aerotow launch failure, getting the nose over during a winch launch failure is even more important. However, use of this technique at lower climb angles yields little benefit and overzealous application at low altitudes could result in diving into the ground.

The question might arise as should the negative Gs be held beyond the peak. Earlier analyses showed that the recovery is enhanced by using higher AoAs (so long as they are still below stall AoA). This argues that the proper time to switch from 0 or negative AoAs is as the glider goes over the top. The precise timing of this transition is not that critical as this will be the lowest airspeed in the recovery and, even if the AoA could be instantly established, the lift is generally low and of little impact on the trajectory.

Density Altitude Effects

Operating at high density altitudes is also of concern particularly for operations high in the mountains. The effect of density altitude is evident in the equation of lift.

$$L = \frac{1}{2} \rho V^2 S \, C_L$$

Elevated density altitude results in the air density, ρ, being lower than for sea-level standard conditions which have been assumed in the previous simulations. For the same AoA (C_L), to generate the same lift, the true airspeed must increase by the $\sqrt{\rho_0 / \rho}$ where ρ_0 is standard sea-level air density. For this illustration, a high density altitude of about 12,000 feet, which can readily occur on hot days in the Colorado Mountains, is assumed. Reference to density altitude converters indicates the air density at this density altitude is about 70% of sea-level and the ratio of true to indicated airspeed is about 1.20. The contour plots will be the same except the horizontal axis and the peak recovery airspeeds will be indicated airspeeds. The true airspeeds will hence be about 20% faster.

Figure 27 presents the height loss contours for operation at 12,000 foot density altitude. The light dashed curves are the reference results at sea-level. The contour interval has been increased to 100 feet to ease interpretation.

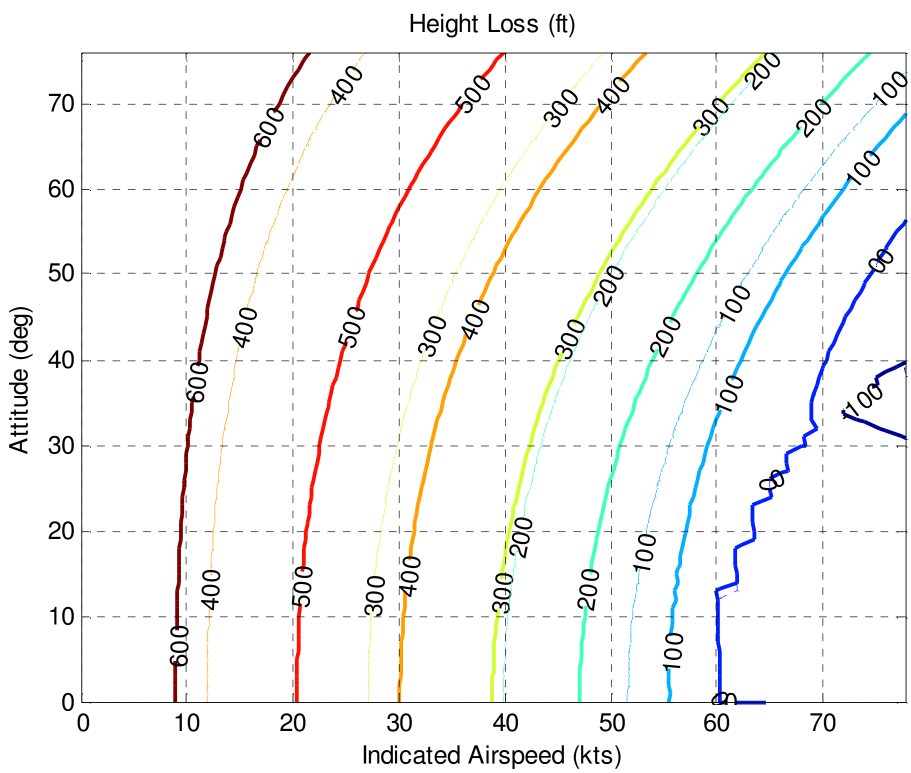

Figure 27. Height Loss Contours for 12,000 Foot Density Altitude.

The height losses, particularly for the lower airspeeds, are substantially greater. As the indicated airspeed increases, the contours converge such that they overlap at the zero height loss contour. The peak airspeed and Gs contours are not included as they exactly overlay so those results are independent of density altitude. The increased height loss with density altitude indicates that extra caution should be exercised when operating at high density altitudes. But operating with appropriate airspeeds still minimizes the reduction of the recoverable AAA envelope.

Summary

This study provides general validation of the concept of immediately unloading the glider into a ballistic trajectory as a key first step in a winch launch failure recovery. A concept for the Dive/Pullout Phase of establishing a constant AoA has provided quantitative guidance to the recoverable Airspeed, Altitude, Attitude (AAA) envelope. Generally having sufficient airspeed has been shown to be far more important than the climb angle (attitude) at the initiation of recovery. Opportunities for higher launches on short runs through the use of tension controlled winces and gliders equipped with AoA indicators were identified. These techniques are not suggested for use with classic winches. Use of higher AoAs was shown to substantially improve the recoverable AAA envelope but with a reduced stall margin. Height losses increase rapidly with higher stall speeds associated with gliders operating at high wing loadings so increased care must be employed. Merit was demonstrated to using negative G pushovers particularly when the recovery is initiated from high climb angles with adequate airspeed. Use of this technique at lower angles/airspeeds is not warranted and over-controlling could be dangerous. Finally, density altitude negatively affects the recoverable AAA envelope but operating at appropriate *indicated* airspeeds minimizes this effect. The key takeaway, airspeed is your friend during the rotation.

References

[1] *Addendum to Rotation Phase Investigation and Consolidated Launch Automation Scheme*. George Moore, 2007.

Appendix

The development of the non-linear differential equations that describe key periods associated with recovery from launch failures is now developed.

Within a certain range of operation, the lift that can be generated by a wing is proportional to the product of the angle-of-attack (AoA) and the airspeed squared. For a given AoA, the lift that is being produced can be reasonably well modeled by the simple equation

$$L = \lambda M\, v^2$$

where λ is a constant of proportionality dependent on wing design and AoA, M is the mass of the aircraft, and v is the airspeed. The reason for explicitly including M will become evident shortly. The ballistic portion of the recovery is not considered in this development but simulations of it using the resulting model is easily accomplished by just setting the parameter λ to zero. The associated differential equations are linear and their solution is well understood. Hence all trajectories in this development will begin with the glider just reaching horizontal flight at the top of the ballistic trajectory segment with a specified airspeed. What is of interest is the trajectory that results for various airspeeds and values of λ corresponding to different values of AoA. The effects of induced and parasitic drag are incorporated later.

The physical model that describes this situation is shown below. The blue trace is that of a glider using a constant AoA pullout. With the elimination of drag, only two forces act on the glider: lift and gravity (weight). Lift is defined to operate perpendicular to the flight path at any instant. Gravity always operates vertically.

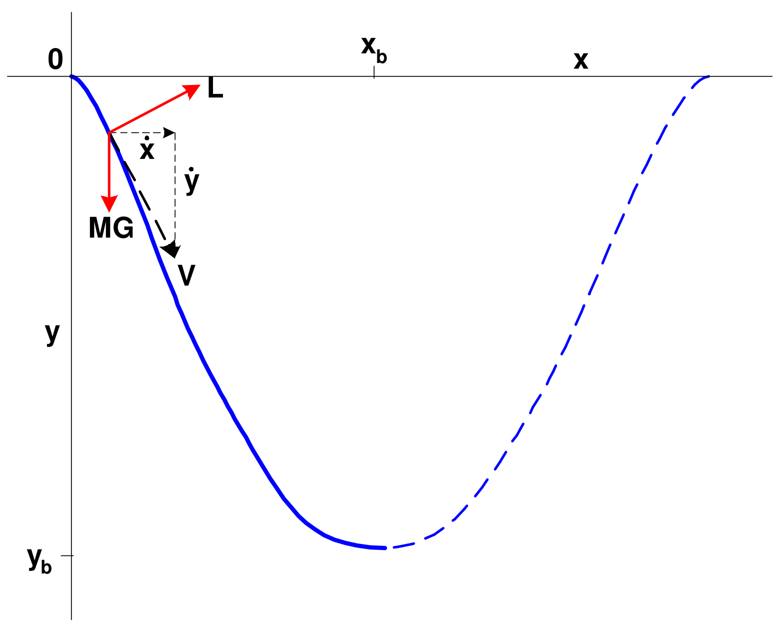

Constant AoA Trajectory Model

Differential equations can be simply defined that describe the flight trajectory using Newton's $F=M\,A$ relation. Initially the analysis will be based on resolving the forces into horizontal and vertical forces but a more elegant mathematical representation will be developed shortly.

The flight trajectory will be described by x, y coordinates. The airspeed, v, is given by

$$v = \sqrt{\dot{x}^2 + \dot{y}^2}$$

where $\dot{x}$ and $\dot{y}$ are the first derivatives of the horizontal and vertical positions respectively, i.e. the horizontal and vertical velocities. The initial conditions for the solutions will be x, y, and $\dot{y}$ equal 0 and $\dot{x}$ equals this peak crossing airspeed.

The angle of the flight trajectory relative to the horizontal, α, is described by

$$\tan(\alpha) = \frac{\dot{y}}{\dot{x}}$$

The horizontal and vertical accelerations are given by resolving the forces yielding

$$\ddot{x} = -\frac{L}{M}\sin(\alpha) = -\frac{\lambda M v^2}{M}\sin(\alpha) = -\lambda v^2 \sin(\alpha)$$

and

$$\ddot{y} = \frac{1}{M}\left(L\cos(\alpha) - G M\right) = \frac{\lambda M v^2}{M}\cos(\alpha) - G = \lambda v^2 \cos(\alpha) - G$$

The reason for including M in the lift relation is now evident as the mass of the aircraft totally drops out of these equations.

Later, when the effects of drag are included, equations and a block diagram for totally algebraic (eliminates the trigonometric functions) representation are developed.

The results of simulations of this equation for different initial airspeeds are shown below. All units employed are SI, for this figure meters.

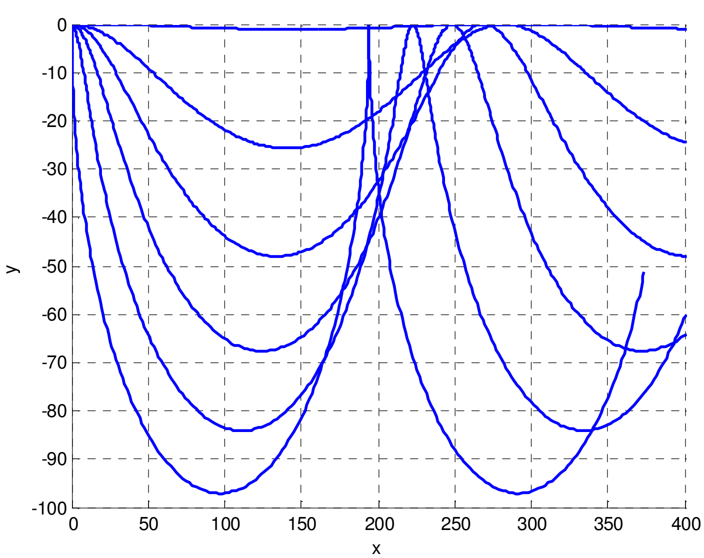

Lossless Flight Trajectories with Different Initial Airspeeds

The airspeeds ranged from 0 to 25 m/s in steps of 5 m/s. The value employed for λ is representative of gliders of interest. Note that the trajectories return to the same height each cycle – a consequence of the lossless model. Very important to pilots is the height lost during the recovery. At zero airspeed over the top, almost 100 m (about 300 feet) was required to recover.

Mathematically, what is more interesting is to observe the behavior of the variables, particularly the velocities, with respect to time. The corresponding horizontal and vertical velocity components and the airspeed are shown below.

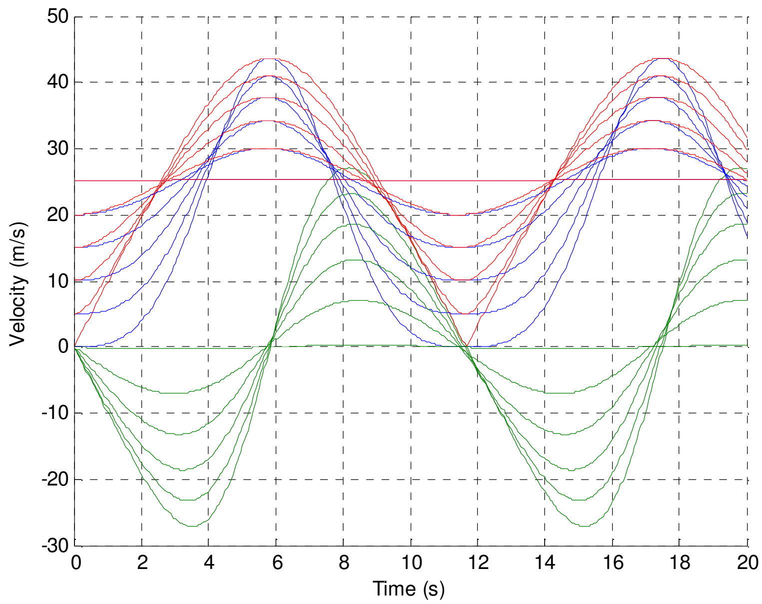

Horizontal (blue), and Vertical (green), and Airspeed (red) Velocities vs. Time

Of particular interest is that the recovery time, the time until the vertical velocity (green) first reaches zero again, is almost invariant of the initial airspeed. Close examination indicates that they are not precisely invariant but very close. The invariance of this period has suggested that a closed-form solution may exist. It also suggests that solutions may be expressed in terms of a Fourier series. The functions are periodic but the effects of the non-linearity are clearly evident in the curves.

A much simpler formulation of the problem may be expressed in the complex domain. If the position is expressed as $z = x + i\,y$, the resulting complex differential equation can take on particularly simple forms. The resulting complex velocity is $v = \dot{z} = \dot{x} + i\,\dot{y}$. When this is put into polar form, the airspeed is the magnitude and the trajectory angle is the phase of v. The underlying first order differential equation can then be expressed as

$$
\begin{aligned}
\dot{v} &= \lambda\,|v|^2\left(-\sin(\alpha) + i\cos(\alpha)\right) - iG \\
&= i\,\lambda\,|v|^2\left(i\,\sin(\alpha) + \cos(\alpha)\right) - iG \\
&= i\,\lambda\,|v|^2\,e^{i\angle v} - iG \\
&= i\,\lambda\,|v|^2\,\frac{v}{|v|} - iG \\
&= i\,\lambda\,|v|\,v - iG
\end{aligned}
$$

λ is still real here but certain forms of drag can be emulated by making this constant complex. Both parasitic and induced drag are proportional to the airspeed squared for a constant AoA. Similarly modeling the drag as

$$D = \delta M v^2$$

the equations become

$$\ddot{x} = \frac{1}{M}\left(-L\sin(\alpha) - D\cos(\alpha)\right) = -v^2\left(\lambda\sin(\alpha) + \delta\cos(\alpha)\right)$$

and

$$\ddot{y} = \frac{1}{M}\left(L\cos(\alpha) - D\sin(\alpha) - GM\right) = v^2\left(\lambda\cos(\alpha) - \delta\sin(\alpha)\right) - G$$

Then,

$$\begin{aligned}
\dot{v} &= |v|^2\left[\lambda\left(-\sin(\alpha) + i\cos(\alpha)\right) + \delta\left(\cos(\alpha) - i\sin(\alpha)\right)\right] - iG \\
&= |v|^2\left[i\lambda\left(\cos(\alpha) + i\sin(\alpha)\right) + \delta\left(\cos(\alpha) - i\sin(\alpha)\right)\right] - iG \\
&= |v|^2\left(\delta + i\lambda\right)e^{i\angle v} - iG \\
&= |v|^2\left(\delta + i\lambda\right)\frac{v}{|v|} - iG \\
&= \left(\delta + i\lambda\right)|v|\,v - iG
\end{aligned}$$

Putting this in the most general and concise form yields

$$\dot{v} = \gamma |v|\, v + \kappa$$

where γ and κ are complex constants.

Alternatively, returning to the pair of coupled non-linear equations, the trigonometric relationship in the horizontal acceleration relation can be eliminated resulting in the algebraic equations

$$\begin{aligned}
\ddot{x} &= -v^2\left(\lambda\sin(\alpha) + \delta\cos(\alpha)\right) \\
&= -\left(\dot{x}^2 + \dot{y}^2\right)\left(\lambda\sin\left(\arctan\left(\frac{\dot{y}}{\dot{x}}\right)\right) + \delta\cos\left(\arctan\left(\frac{\dot{y}}{\dot{x}}\right)\right)\right) \\
&= -\left(\dot{x}^2 + \dot{y}^2\right)\left(\lambda\frac{\dot{y}}{\sqrt{\dot{x}^2 + \dot{y}^2}} + \delta\frac{\dot{x}}{\sqrt{\dot{x}^2 + \dot{y}^2}}\right) \\
&= -\sqrt{\dot{x}^2 + \dot{y}^2}\left(\lambda\dot{y} + \delta\dot{x}\right)
\end{aligned}$$

or

$$\ddot{x} = -v\left(\lambda\dot{y} + \delta\dot{x}\right)$$

Similarly, the vertical acceleration can be expressed as

$$\ddot{y} = \sqrt{\dot{x}^2 + \dot{y}^2}\,(\lambda\,\dot{x} - \delta\,\dot{y}) - G$$

or

$$\ddot{y} = v\,(\lambda\,\dot{x} - \delta\,\dot{y}) - G$$

A block diagram suitable for simulation follows where $\frac{1}{s}$ is the Laplace transform representation for integration.